AMERICAN UNIVERSITY OF BEIRUT

# NEUROPROTECTIVE EFFECT OF MITOQUINONE ON HYDROGEN PEROXIDE-INDUCED NEUROTOXICITY IN SH-SY5Y NEUROBLASTOMA CELLS

by
CHLOE AMINE BARSA

A thesis
submitted in partial fulfillment of the requirements
for the degree of Master of Biochemistry
to the Department of Biochemistry and Molecular Genetics
of the Faculty of Medicine
at the American University of Beirut

Beirut, Lebanon
April 2022

AMERICAN UNIVERSITY OF BEIRUT

# NEUROPROTECTIVE EFFECT OF MITOQUINONE ON HYDROGEN PEROXIDE-INDUCED NEUROTOXICITY IN SH-SY5Y NEUROBLASTOMA CELLS

by

CHLOE AMINE BARSA

Approved by:

| | |
|---|---|
| Dr. Firas Kobaissy, Associate Professor<br>Department of Biochemistry and Molecular Genetics | Signature Nadine Darwiche on behalf of Dr. F. Kobaissy<br>Advisor |
| Dr. Nadine Darwiche, Professor<br>Department of Biochemistry and Molecular Genetics | Signature Nadine Darwiche<br>Co-Advisor |
| Dr. Aida Habib Abdul Karim, Professor<br>Department of Biochemistry and Molecular Genetic | Signature Nadine Darwiche on behalf of Dr. Aida Habib<br>Member of Committee |
| Dr. Wassim Abou Kheir, Associate Professor<br>Department of Anatomy, Cell Biology and Physiology | Signature<br>Member of Committee |
| Dr. Riyad El-Khoury, Assistant Professor<br>Department of Pathology and Laboratory Medicine | Signature<br>Member of Committee |

Date of thesis defense: April 29, 2022

# AMERICAN UNIVERSITY OF BEIRUT

## THESIS RELEASE FORM

Student Name: ____BARSA_____CHLOE_____AMINE___
Last First Middle

I authorize the American University of Beirut, to: (a) reproduce hard or electronic copies of my thesis; (b) include such copies in the archives and digital repositories of the University; and (c) make freely available such copies to third parties for research or educational purposes:

☐ As of the date of submission

☒ One year from the date of submission of my thesis.

☐ Two years from the date of submission of my thesis.

☐ Three years from the date of submission of my thesis.


Signature Date

# ACKNOWLEDGEMENTS

I would first like to express my sincere gratitude to my advisor, Dr. Firas Kobaissy, for the continuous support, guidance and motivation that he has been giving me during my master's research.

Also, I would like to thank my co-advisor, Dr. Nadine Darwiche as well as her lab manager, Berthe Hayar, for their continuous help, kindness and guidance for without them, the completion of my master's might not have been possible.

My sincere thanks also go to the rest of my committee members: Dr. Wassim Abou Kheir for his continuous follow-up and comprehensive advice, Dr. Aida Habib Abdul Karim for her wisdom and broad support and Dr. Riyad El Khoury for his help and counsel.

Also, I take this opportunity to record my sincere gratitude to Dr. Julnar Usta for always supporting me.

I would also like to thank my fellow lab members (Sarin, Judith, Mohammad, Muhammad Ali, and Mark) for their continuous support and their help as well as my friends, both from and outside the department, for they have always been there on both good and bad days.

I would also like to acknowledge last but not least all the core-facility members of the department for their help, for without them, research at DTS wouldn't even be possible.

# ABSTRACT

# OF THE THESIS OF

Chloe Amine Barsa for Master of Science
Major: Biochemistry

Title: Neuroprotective Effect of Mitoquinone on H2o2-Induced Neurotoxicity in Sh-Sy5y Neuroblastoma Cells

Several studies have investigated the major role that oxidative stress plays in the pathogenesis of traumatic brain injury (TBI). In fact, reactive oxygen species (ROS) accumulation, one major constituent of the secondary injury of TBI, has been shown to contribute to the processes of neuroinflammation, apoptosis, autophagy, and mitochondrial dysfunction, all of which are common characteristics of brain injury profile. The Nrf2-Keap1-ARE pathway is one particular pathway that has been of specific interest to researchers with several studies revealing its implication in TBI pathology. The possibility of targeting this pathway, using antioxidant compounds, has been proposed as a potential neurotherapy for TBI. Among these compounds is mitoquinone (MitoQ), an antioxidant that has been shown to exhibit a neuroprotective effect on both closed and open head injury models of TBI *in vivo*.

The goal of this study is to investigate the potential effect of MitoQ, an antioxidant drug that targets the mitochondria, on neurotoxicity induced by hydrogen peroxide ($H_2O_2$) in humans neuroblastoma SH-SY5Y cells as an *in vitro* model of oxidative stress.

The neuroprotective effect of mitoquinone on SH-SY5Y cells was assessed by MTT assay (for cell viability), SRB assay (for cell growth inhibition), and propidium iodide stain (for cell cycle) using two different concentrations of the drug (0.03 µg/mL and 0.05 µg/mL) as a pre-treatment and post-treatment for H2O2-induced stress. Oxidative stress was evaluated by NBT assay and DHE staining while mitochondrial integrity was studied using MitotrackerGreen Fluorescent dye. Finally, the gene expression profile of selected antioxidant genes (Nrf2, SOD, HMOX1, and CAT genes) and inflammatory genes (COX-2 and NFκB) were investigated via RT-qPCR or immunofluorescence imaging.

Our results showed that pre-treatment with the drug MitoQ protects SH-SY5Y cells by increasing cell viability, decreasing cell growth inhibition, preserving cell morphology and cell cycle integrity and attenuating oxidative stress progression. Moreover, mitochondrial phenotype was preserved in cells treated with MitoQ prior to $H_2O_2$ stress-induction. The Nrf2-Keap-ARE was shown to be contributing to the protective effects of MitoQ with an upregulation of the antioxidant genes Nrf2 and HOX1 and a normalization of SOD1 gene expression. Also, the decrease in COX-2 levels indicates the anti-inflammatory effect of the antioxidant which supports even more the use of MitoQ as treatment for neurotoxicity.

TABLE OF CONTENTS

# ILLUSTRATIONS

Figure

# TABLES

Table

# ABBREVIATIONS

**A**

AR: aspect ratio

ARE: antioxidant response element

**B**

BBB: blood brain barrier

**C**

CAT: catalase

CBF: cerebral blood flow

COX-2: cyclooxygenase-2

Cyt c: cytochrome c

**D**

ddH2o: double distilled water

DHE: dihydroethidium

DMSO: dimethylsulfoxide

**F**

FBS: Fetal bovine serum

FDA: Food and Drug Administration

**G**

GPX: glutathione peroxidase

**H**

$H_2O_2$: hydrogen peroxide

HMOX: heme oxygenase

**I**

ICC: immunocytochemistry

IL-6 : interleukin-6

**K**

KOH: potassium hydroxyde

**M**

MitoQ: mitoquinone

MTT: 3-(4,5-dimethyl-thiazol-2yl)-2,5-diphenyl tetrazolium bromide

**N**

NFκB: nuclear factor kappa-light-chain-enhancer of activated B cells

NQO1: NAD(P)H quinone dehydrogenase 1

Nrf2: Nuclear factor erythroid 2-related factor 2

**P**

PBS: phosphate-buffered saline

PBST: PBS-Tween

PFA: paraformaldehyde

**R**

RNS: reactive nitrogen species

ROS: reactive oxygen species

RT-qPCR: quantitative real-time polymerase chain reaction

**S**

SDH: succinate dehydrogenase

SOD: superoxide dismutase

SRB: Sulforhodamine B

**T**

TBI: traumatic brain injury

TCA: trichloroacetic acid

TNFα: tumor necrosis factor alpha

TPP: triphenylphosphonium

# CHAPTER 1
# INTRODUCTION

## 1.1. Traumatic Brain Injury

Traumatic brain injury, commonly referred to as TBI, is defined as an acquired brain damage resulting from sudden trauma to the brain that disrupts the normal function of the brain (Capizzi, Woo, & Verduzco-Gutierrez, 2020). TBI is a common health condition that affects the lives of many worldwide, the global incidence of TBI being estimated at 939 cases per 100,000 individuals (Dewan et al., 2018).

### *1.1.1. A heterogeneous disease*

An important characteristic of TBI is its heterogeneity. In fact, several factors contribute to the wide spectrum of injury severity reflected in the short-term and long-term symptoms that the TBI victim will experience (Senoner & Dichtl, 2019), the two main factors being the intensity of the impact and the area of the brain that is affected.

Most medications given to TBI patients aim to alleviate the burden of the disease by targeting some of the symptoms resulting from the injury, whether they are physical, cognitive, or behavioral symptoms (Devi et al., 2020; Dikmen et al., 2009; Fann, Katon, Uomoto, & Esselman, 1995).

However, to this day, because of the limited knowledge that we have of the underlying pathophysiological mechanisms of TBI, there are no Food and Drug Administration (FDA)-approved drugs for treating this chronic disease, the heterogeneous aspect of TBI hindering the discovery or/and design of a cure.

### *1.1.2. From primary to secondary injury*

The resulting neurological and cognitive complications in TBI stem from the coordination between two events known as the primary brain injury and the secondary injury.

The primary injury is the direct result of the external physical force on the brain; it is considered to be more or less complete at the time of the impact. It is mainly characterized by direct tissue damage and disruption of cerebral blood flow (CBF) and metabolism (Werner & Engelhard, 2007).

On the other side, secondary injury refers to the changes that evolve over a period of minutes, hours and days following the primary injury and consists of cellular, molecular and chemical changes that will contribute to further brain tissue destruction and neuronal damage (Borgens & Liu-Snyder, 2012). Inflammation, mitochondrial dysfunction, excitotoxicity, and oxidative stress are some of those secondary cellular injury mechanisms (Greve & Zink, 2009) that will exacerbate cognitive dysfunction by enhancing synaptic dysfunction, cell death and axonal degeneration (figure 1).

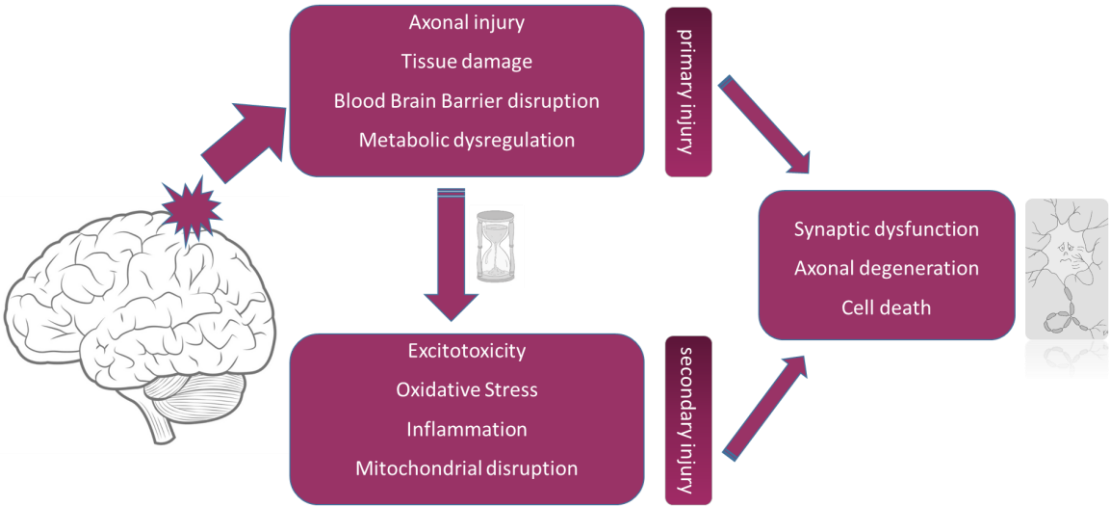


Figure 1 TBI pathophysiology: from primary to secondary injury.

## 1.2. Oxidative Stress

Research over the years have revealed the crucial role that reactive oxygen species (ROS) and reactive nitrogen species (RNS) play in numerous physiological as well as pathophysiological processes in the human body (D'Autreaux & Toledano, 2007; Martinez & Andriantsitohaina, 2009).

### *1.2.1. Definition and outcomes*

It is now well-established that oxidative stress and nitrosative stress which result from an imbalance between the antioxidant system and the oxidant system (Pizzino et al., 2017) are involved in many pathological conditions such as cancer (Prasad, Gupta, & Tyagi, 2017), cardiovascular diseases (Senoner & Dichtl, 2019) and hypertension (Datla & Griendling, 2010).

This imbalance which leads to ROS and/or RNS accumulation can result either from a greater production of such highly reactive molecules, or from the malfunctioning of the endogenous antioxidant machinery, if not a combination of both.

Oxidative stress will cause inflammation, apoptosis, autophagy, neuronal dysfunction as well as mitochondrial disruption (Elsayed Azab et al., 2019) (figure 2), all of these cellular processes being common players in numerous diseases, TBI being one of them.

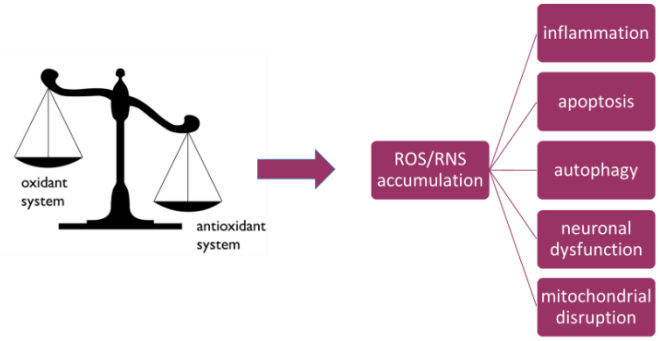


Figure 2 Major mechanisms of oxidative stress.

### *1.2.2. Role of Oxidative Stress in TBI pathology*

Following injury, the brain will encounter an increase in ROS levels as a result of abnormal cellular metabolism and respiration. And because neuronal cells are characterized by their polyunsaturated fatty acids-rich membrane and their weak antioxidant defense (X. Wang & Michaelis, 2010), oxidative stress is considered to be the main contributor to the pathophysiology of TBI.

In fact, this oxidative stress will induce mitochondrial dysfunction, lipid peroxidation as well as damage in proteins and nucleic acids (Nakagawa et al., 2005) which will slow down and eventually impair brain reparation.

## 1.3. The Nrf2-Keap-ARE pathway

One particular pathway related to oxidative stress that has been of a specific interest for researchers these past few years is the Nrf2 (Nuclear factor erythroid 2-related factor 2)-Keap1-ARE pathway.

### *1.3.1. Importance of the pathway*

The Nrf2-Keap-ARE pathway has been shown to regulate the expression of numerous cyto-protective genes including but not limited to antioxidant genes, genes encoding enzymes that participate in glutathione synthesis and glutathione regeneration and genes encoding detoxifying molecules (Harvey et al., 2009; Tu, Wang, Li, Liu, & Sha, 2019).

To name a few of those Nrf2-regulated genes are heme oxygenase-1 (HMOX1), NAD(P)H quinone dehydrogenase 1 (NQO1), catalase (CAT) and superoxide dismutase (SOD) (H. Zhu, Itoh, Yamamoto, Zweier, & Li, 2005) which have anti-inflammatory, anti-apoptotic and anti-oxidative properties.

### *1.3.2. Nrf2 and oxidative stress*

Under stressful conditions, in which electrophiles and oxidants switch on the Nrf2-dependent cellular defense mechanism, Nrf2 is released from Keap1 and will translocate to the nucleus where it binds to the conserved ARE (antioxidant response element) sequence (Ma, 2013).

The translocation of Nrf2 will induce the transcription of many cytoprotective genes which will help in decreasing ROS/RNS levels (Ma, 2013) and inhibiting the harmful downstream events that will result from oxidative stress (figure 3).

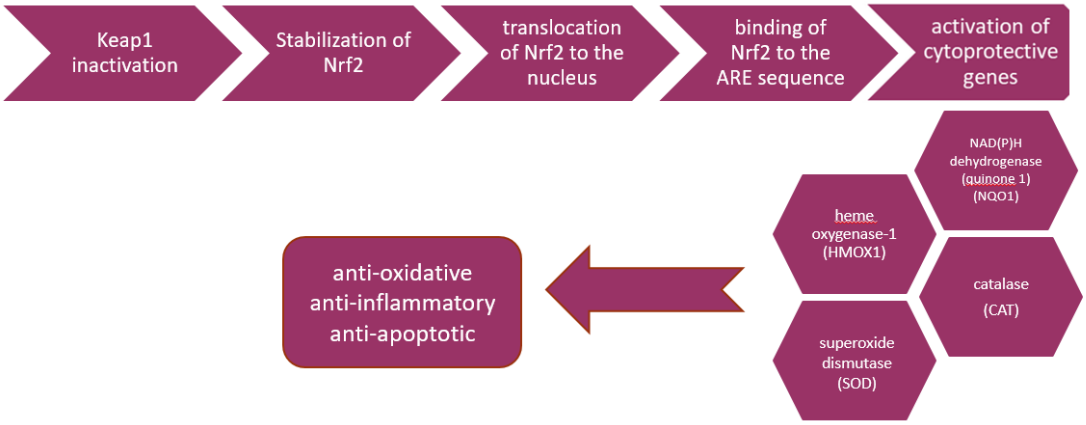


Figure 3 Nrf2-Keap-ARE pathway's response to oxidative stress.

## 1.4. Antioxidants

Because oxidative stress plays a crucial role in TBI pathology, scientists are increasingly investigating many mitochondria-targeted antioxidants and their potential ROS/RNS-scavenging properties to slow down TBI's progression (Davis & Vemuganti, 2022).

### *1.4.1. Structure of Mitoquinone (MitoQ)*

Mitoquinone (MitoQ) also known as 10-(4,5-Dimethoxy-2-methyl-3,6-dioxo-1,4-cyclohexadien-1-yl)decyl triphenyl phosphonium methanesulfonate, seen in figure 4, is one of those mitochondria-targeted antioxidant that have been of specific interest for scientists this past decade (Smith & Murphy, 2010).

This safe antioxidant results from the covalent attachment of the endogenous antioxidant ubiquinone to a lipophilic triphenylphosphonium (TPP+) cation (Davis & Vemuganti, 2022). Such structure allows better absorption of the compound by the blood-brain barrier (BBB) and by neuronal membranes facilitating its accumulation in the mitochondria and therefore increasing its potency (Kelso et al., 2001).

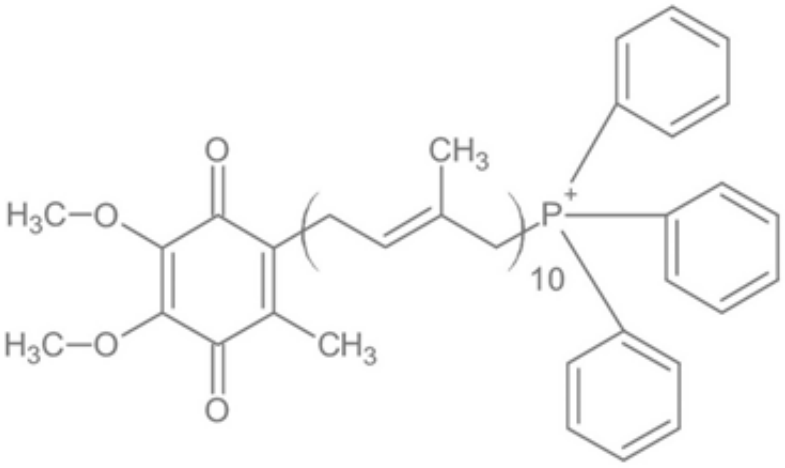


Figure 4 Chemical structure of the mitochondrial antioxidant mitoquinone (MitoQ).

Following its entrance into the inner mitochondrial membrane, ubiquinone will be reduced by the respiratory complex II or succinate dehydrogenase (SDH) to the active lipid-soluble antioxidant ubiquinol. The latter will scavenge ROS and protect cells from further damage (James et al., 2007).

### *1.4.2. MitoQ and the Nrf2 pathway*

Both *in vivo* and *in vitro* studies have revealed that the neuroprotective activity of MitoQ is related to the Nrf2-Keap-ARE pathway (Cen et al., 2021; Rao et al., 2010).

In fact, this ubiquinone derivative appears to increase Nrf2 expression which in turn increases the expression of antioxidant enzymes such as superoxide dismutase (SOD), glutathione peroxidase (GPX) and heme oxygenase (HMOX) (Li et al., 2019).

It has also been shown that MitoQ has anti-inflammatory properties and is able to decrease tumor necrosis factor-alpha (TNFα) levels and interleukin 6 (IL-6) levels (Powell et al., 2015) as well as other cytokines. Moreover, MitoQ has been shown to prevent cytochrome c (Cyt c) release and inhibit caspase-3 activation (Wani et al., 2011). The latter will impede mitochondrial-dependent apoptosis, supporting the use of such antioxidant to limit neurotoxicity buildup and cell death following TBI.

## 1.5. An *in vitro* model

Recently, significant advances have been made in the experimental studies of many neurodegenerative diseases *in vitro* counting TBI through the use of cell models including but not limited to tumor-derived-, neuronal- and immortalized cell lines (Heusinkveld & Westerink, 2017).

### *1.5.1. SH-SY5Y cell line*

SH-SY5Y cells are neuroblastoma cells that are derived from the SK-N-SH cell subline derived from a metastatic bone marrow biopsy in 1970.

They can be cultured either as adherent cells or as floating cells and can be differentiated into more neuron-like cells expressing specific human neuronal markers through a variety of different mechanisms and chemicals (Kovalevich & Langford, 2013).

Undifferentiated SH-SY5Y cells (seen in figure 5) are characterized by a neuroblast-like, epithelial morphology and a doubling time of around 48 hours. They tend to form clusters of non-polarized neuroblastic cells with many short and truncated processes (Kovalevich & Langford, 2013).

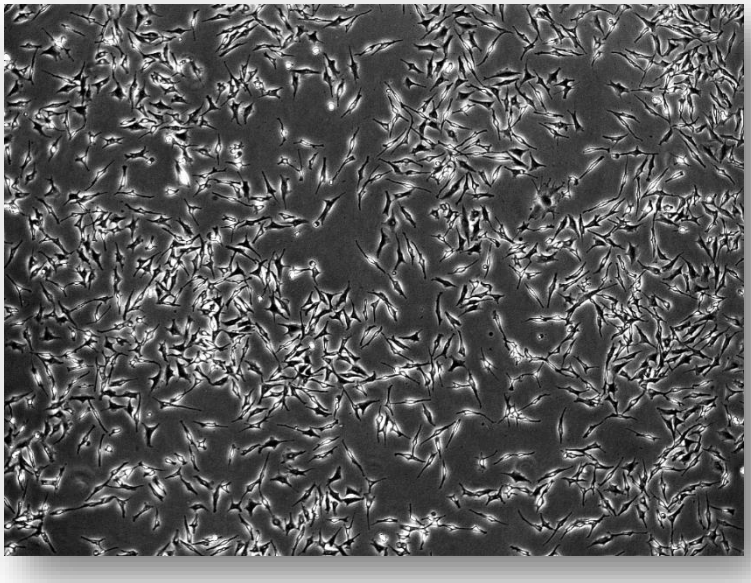

Figure 5 Cell morphology of undifferentiated SH-SY5Y neuroblastoma cells

Exhibiting neuronal enzyme activity with non-negligible levels of tyrosine and dopamine-β-hydroxylase being measured even before differentiation, undifferentiated SH-SY5Y cells have been widely used as a neuronal model since the 80s (Xie, Hu, & Li, 2010) and are, to this day, widely used as an *in vitro* model to investigate the underlying molecular mechanisms and the corresponding therapeutic targets of several brain diseases (Forster et al., 2016).

### *1.5.2. Mimicking neurotoxicity in vitro*

Hydrogen peroxide ($H_2O_2$), which is one of the naturally produced non-radical ROS that is generated by mitochondrial respiration, is often used as an experimental source of ROS (Aruoma & Halliwell, 1987).

In fact, after readily crossing the cell membrane, $H_2O_2$ will be converted to more toxic hydroxyl radicals via catalysis which will further induce oxidative stress (Halliwell & Gutteridge, 1984).

Hence, $H_2O_2$ treatment of culture neuroblastoma cells can and has been employed to mimic neurotoxicity *in vitro* (Fujita et al., 2006; C. M. Wang, Yang, Cheng, Chen, & Bai, 2018; Wei, Tian, Yan, Shao, & Xie, 2014) and more importantly will allow us to replicate the oxidative stress that most brain diseases, including TBI, sustain.

# CHAPTER 2

# HYPOTHESIS AND AIMS OF THE STUDY

Reactive oxygen species (ROS) accumulation plays a crucial role in TBI pathogenesis which is facilitated by the selective neuronal vulnerability to oxidative stress. And because the respiratory organelle is the main source of ROS, investigating the ROS scavenging properties of mitochondrial-targeted antioxidants such as mitoquinone (MitoQ) has become of special interest to many researchers.

## 1. Hypothesis of the study

In this study, we hypothesize that the mitochondria-targeted antioxidant mitoquinone (MitoQ) has beneficial effects in reducing oxidative stress by targeting the Nrf2-ARE pathway and may therefore be considered a potential treatment for neurotoxicity.

## 2. Aims of the study

Six aims were set to test the hypothesis.

***Aim 1:***

Induction of oxidative stress and neurotoxicity on SH-SY5Y neuroblastoma cells by treatment with $H_2O_2$.

***Aim 2:***

Evaluation of the neuroprotective effect of MitoQ by assessing cell viability/cell death and cell integrity as well as cell cycle regulation.

***Aim 3:***

Assessment of the neuroprotective effect of MitoQ by investigating oxidative stress.

***Aim 4:***

Examining the involvement of the mitochondria in the protective role of MitoQ.

***Aim 5:***

Understanding the implication of the Nrf2 pathway in the inferred protection by MitoQ.

***Aim 6:***

Examining the anti-inflammatory property of MitoQ.

# CHAPTER 3

# MATERIALS AND METHODS

## 2.1. Cell Culture

SH-SY5Y human neuroblastoma cell line (CRL-2266) was purchased from the American Type Culture Collection (ATCC, Manassas, VA, USA). The semi-adherent epithelial-like cells were cultured in Dulbecco's Modified Eagle's Medium/Nutrient Mixture F-12 Ham medium (Sigma-Aldrich, USA; D8437) supplemented with 10% Fetal Bovine Serum (FBS) (Sigma-Aldrich, USA; F9665) and 1% Penicillin-Streptomycin mixture (Lonza, USA; DE17-602E) at 37 °C in an incubator with a humidified atmosphere of 5% $CO_2$.

Reaching 80% confluency, they were passaged by trypsinization using TrypLE™ Express Enzyme (1X) (Gibco, USA; 12604013) and were seeded into 12-well, 24-well or 96-well plates depending on the experiment.

## 2.2. Mitoquinone Supplementation

Mitoquinone (Focus Biomolecules, Philadephia, USA; 10-1365; MW=663.64) also known as 10-(6′-Ubiquinonyl)decyltriphenylphosphonium bromide was dissolved in 100 µL of dimehtylsulfloxide (DMSO) (Sigma-Aldrich, USA; D8418). Then, 900 µL of phosphate-buffered saline (1x) (PBS) was added to attain a concentration of 25 mg/mL.

### 2.3. Cell Treatment

Seeded cells were allowed to attach for 18 hours before adding the specific treatments. Oxidative stress induction was accomplished by treating the cells for 24 hours with hydrogen peroxide ($H_2O_2$) after the 24-hours incubation period with MitoQ for pre-treatment, and before the 24-hours incubation period with MitoQ for post-treatment.

The dosage of 100 µM of $H_2O_2$ was opted for inducing stress based on MTT cell viability results after testing the effect of different $H_2O_2$ concentrations ranging from 0µM to 300µM at t=24 hours, t=48 hours and t=72 hours (figure 6). The different $H_2O_2$ dosages were prepared by dilution of the stock solution of hydrogen peroxide 30% (Sigma-Aldrich, USA; 18312) directly into the complete media.

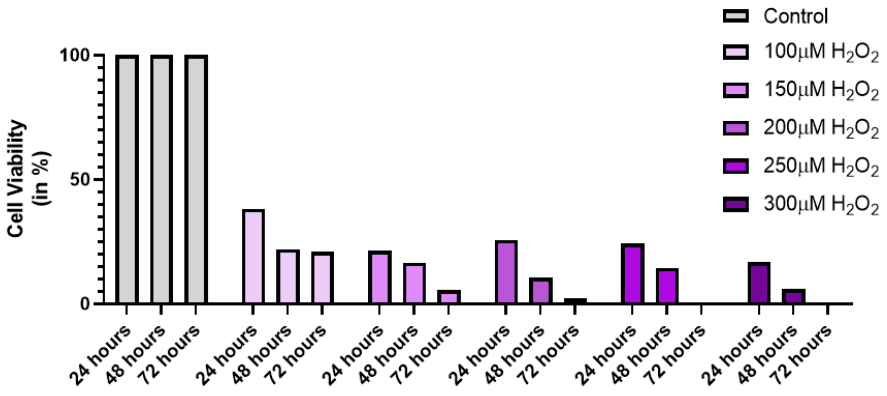


Figure 6 Assessing $H_2O_2$-induced toxicity via MTT assay.

Values obtained from 3 experiments (performed in triplicates) are described as mean ± S.E.M.

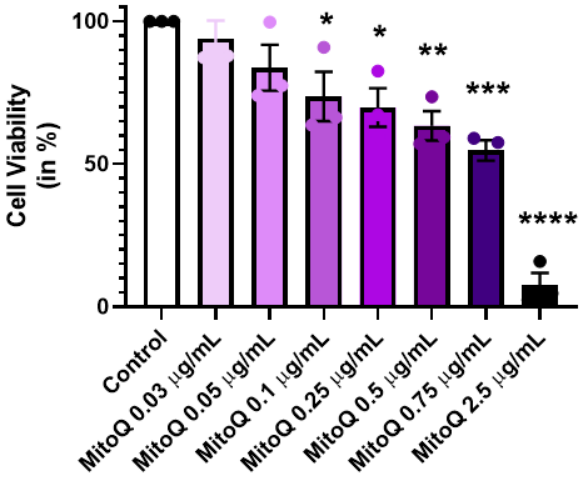


Figure 7 Assessing MitoQ-induced toxicity via MTT assay.

Values obtained from 3 experiments (performed in triplicates) are described as mean ± S.E.M.
Statistics: ANOVA with Dunnet's Multiple Comparison post hoc test: *p < 0.05, **p < 0.01,***p < 0.001

Two concentrations of MitoQ (0.03 µg/mL and 0.05 µg/mL) were incubated into SH-SY5Y cells; both dosages were determined to be safe using MTT assay (figure 7).

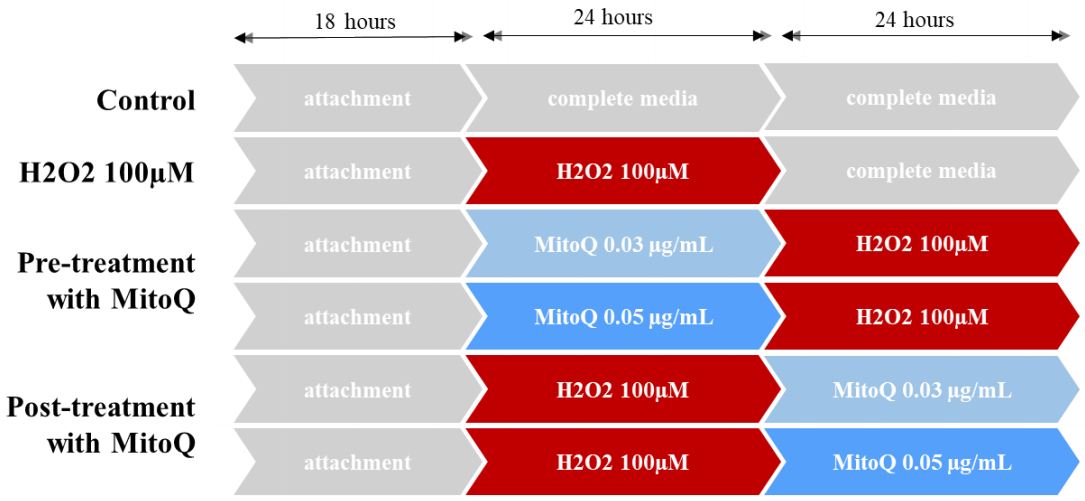


Table 1 Different treatment conditions of SH-SY5Y cell culture.

Six treatment conditions (seen in table 1) were established and studied.

### 2.4. Cell viability measurement

Cell viability was assessed by reduction of 3-(4,5-dimethyl-thiazol-2yl)-2,5-diphenyl tetrazolium bromide (MTT) by NAD-dependent dehydrogenase activity which results in the formation of an insoluble dark blue MTT-formazan (Kumar, Nagarajan, & Uchil, 2018).

Briefly, SH-SY5Y cells were seeded onto 96-well plates at a density of 5,000 cells in 100 µL per well. The cells were then incubated with the different treatments for a total of 48 hours after which 10 µL of MTT solvent (prepared in PBS at the concentration of 0.5 mg/mL) was added to each well. The plates were incubated for an additional 3 hours at 37 °C before adding, in each well, 100 µL of MTT stop solution for the formazan

products to be dissolved. The absorbance of each well was obtained the next day using a microplate spectrophotometer set at 595 nm.

The experiment was carried out in quadruplicates and percentage cell viability was calculated as shown below:

$$\%\ cell\ viability = \left(\frac{absorbance\ of\ treated\ cells - absorbance\ of\ blank}{absorbance\ of\ untreated\ cells - absorbance\ of\ blank}\right) \times 100$$

### 2.5. Cell growth inhibition measurement

After 48 hours of specific and respective treatments, SH-SY5Y seeded at 5,000 cells per well in 96-well plates were fixed using cold trichloroacetic acid (TCA) solution and then washed with ddH2O and allowed to dry overnight. The next day, 50 µL of 0.04% Sulforhodamine B (SRB) solution was added to each well and was followed by washing with 1% acetic acid and then drying. Lastly, 100 µL of Tris base solution was added to allow dissociation of the stoichiometrically bounded proteins and absorbance was determined using a microplate spectrophotometer set at 510 nm.

The experiment was carried out in triplicates and cell growth inhibition was calculated as shown below:

$$\%\ growth\ inhibiton = 100 - \left(\frac{absorbance\ of\ treated\ cells - absorbance\ of\ blank}{absorbance\ of\ untreated\ cells - absorbance\ of\ blank} \times 100\right)$$

### 2.6. Cell cycle analysis

SH-SY5Y cells seeded at 60,000 cells per well in a 12-wells plate and treated were collected, washed twice with ice-cold 1x PBS and fixed with 70% cold ethanol for 40min. Afterwards, they were incubated at 37 °C for 30 minutes in 200 µL of 1X PBS buffer containing 10 µg/mL RNase A and 5 µg/mL propidium iodide.

Following staining, the cells were washed and the percentage of cells at various cell cycle phases was determined using the flow cytometer. The experiment was carried out in quadruplicates and the obtained data was analyzed using the Diva software.

### 2.7. Oxidative Stress Assessment

The formation of reactive oxygen species (ROS) was evaluated using the cell-permeable fluorogenic probe dihydroethidium (DHE) on SH-SY5Y cells seeded at a density of 20,000 cells per well in 24-well plates on glass coverslips.

After appropriate treatment administration and incubation time, the cells are fixed using 4% paraformaldehyde (PFA) and then permeabilized. After that, incubation in the dark for 40 minutes in 400 µL of DHE working solution was achieved, followed by a few washes with PBS (1X). All coverslips were mounted using DAPI-mounting solution and the samples were viewed under fluorescent microscopy; the experiment was done in triplicates.

DHE working solution was prepared by diluting 1uL of the 5mM solution (Invitrogen, USA; D23107) in 1 mL of PBS (1X).

### 2.8. ROS levels measurement

Nitroblue tetrazolium (NBT) reduction assay was used to assess the ROS content, with the formation of blue-black compounds called formazon following NBT reduction by free oxygen radicals (Choi, Kim, Cha, & Kim, 2006).

After growing and treating the cells with their respective treatments in 96-well plates, 100 µL of the 1mg/mL NBT working solution was added to each well. After an hour of incubation in the yellow dye, washing with 100% methanol was achieved. Then,

120 µL of 2M potassium hydroxide (KOH) solution and 140 µL of DMSO were added to the air-dried plate. Absorbance was determined using a microplate spectrophotometer set at 630 nm.

The experiment was carried out in quadruplicates and relative ROS production was calculated as shown below:

$$\%\ \text{ROS proudction} = 100 - \left(\frac{absorbance\ of\ treated\ cells - absorbance\ of\ blank}{absorbance\ of\ untreated\ cells - absorbance\ of\ blank} \times 100\right)$$

### 2.9. Mitochondrial morphology

The fluorescent mitochondrial stain Mitotracker Green FM was used to assess mitochondrial vital activity.

Briefly, treated SH-SY5Y cells that were seeded on coverslips at a density of 20,000 cells per well in 24-well plates, were washed with PBS (1X). The cells were incubated in 400 µL of the working solution for 35 min in the dark.

All coverslips were mounted using a DAPI-mounting solution after some additional washes with PBS (1X) and the samples were viewed under fluorescent microscopy; the experiment was done in triplicates.

MitotrackerGreen working solution was prepared by dilution of the stock MitotrackerGreen FM (Invitrogen, USA; M7514) in PBS (1X) to reach the final concentration of 200 nM.

### 2.10. Quantitative real-time PCR

RNA was extracted from SH-SY5Y cells seeded and treated in triplicates in 12-well plates at a density of 50,000 cells per well using Trizol (Sigma-Aldrich, USA; T9424).

RNA was then purified using TURBO DNA-free Kit (Invitrogen, USA; AM1907) and 1.5 µg of RNA were transcribed using the 5X iScript cDNA synthesis kit in a thermal cycler using the following protocol: priming at 25°C for 5 minutes, then reverse transcription at 46°C for 25 minutes, followed by RT inactivation at 95°C for 1 minute.

Quantitative real-time PCR was then applied to 2.5 µL of cDNA (equivalent to 50 ng of cDNA) using the 4X CAPITAL™ qPCR Green Master Mix (Biotechrabbit, Germany; BR0501703) and 10µM of each of the reverse and forward primers.

Cycling conditions were as follows: 95°C for 3 minutes for one cycle, then 95°C for 15 seconds followed by annealing at 60°C for 30 seconds for 55 cycles, and finally 72°C for 5 minutes for one cycle. The primers used are listed in the table found right below

| **Gene Targeted** | **Forward Primer (5' – 3')** | **Reverse Primer (5' – 3')** |
|---|---|---|
| Nrf2 | CAGCGACGGAAAGAGTATGA | TGGGCAACCTGGGAGTAG |
| SOD1 | ACAGGCCTTATTCCACTGCT | CAGCATAACGATCGTGGTTT |
| CAT | GATAGCCTTCGACCCAAGCA | ATGGCGGTGAGTGTCAGGAT |
| HMOX1 | ATGACACCAAGGACCAGAGC | GTGTAAGGACCCATCGGAGA |
| COX-2 | TGCTGGCAGGGTTGCTGGTGGTA | GGGCTTCAGCATAAAGCGTTTGCGG |
| GAPDH | ACCCACTCCTCCACCTTTGA | CTGTTGCTGTAGCCAAATTCGT |

Table 2 Different primer sequences used to determine relative gene expression by RT-qPCR

### 2.11. Immunocytochemistry (ICC)

Following fixation with PFA 4% for 30 minutes and permeabilization using 0.5% PBS-Triton X solution for 40 minutes, the treated cells were incubated in 400 µL of blocking solution for 90 minutes at room temperature.

The cells were then incubated overnight at 4 °C with primary antibodies diluted in the blocking solution. The primary antibodies used were anti-βIII-tubulin (dilution of 1:400; Sc -588888; Santa Cruz), anti- Nrf2 (dilution of 1:400; ab31163; Abcam) and anti-NFκB p65 (dilution of 1:400; D14E12; Cell Signaling). Then, prior to the hour-long incubation with secondary antibodies, the fixed cells are washed with 0.1% PBS-Tween (PBST). The secondary antibodies used were goat anti-chicken IgG H&L (Alexa Fluor® 647) (dilution of 1:1000; 115-605-146; Invitrogen) and goat anti-rabbit IgG H&L (Alexa Fluor® 568) (dilution of 1:1000; ab175696; Abcam) respectively. Two washes with PBST were completed before mounting the coverslips using a DAPI-mounting solution.

Images were acquired by confocal imagery as Z-stacks with 40× oil objectives and analyzed using the Zeiss ZEN 2009 image analysis software and NIH ImageJ program. The experiment was done in triplicates.

### 2.12. Statistical Significance

Data analysis was performed using Graph Pad Prism 8.4.3 (Graph Pad Software Inc., USA). One-way ANOVA test was used to compare the mean differences across all treatments while Welch's test or Dunnet's test was used for comparison between two specific treatments. Differences were considered to be statistically significant at $p < 0.05$: *** ($p < 0.001$), ** ($p < 0.01$), * ($p < 0.05$).

# CHAPTER 4

# RESULTS

### 3.1. Pre-treatment with MitoQ improves cell viability and suppresses cell growth inhibition

MTT assay analysis (figure 7) shows that pre-treatment with MitoQ at both concentrations significantly increased the viability of $H_2O_2$-stressed cells from 47.8% to 57.7 % at 0.03 µg/mL and from 47.8% to 66.5% at 0.05 µg/mL.

However, post-treatment with MitoQ did not induce a significant effect on the viability of the $H_2O_2$-treated cells even though an increase in viability seems to be present.

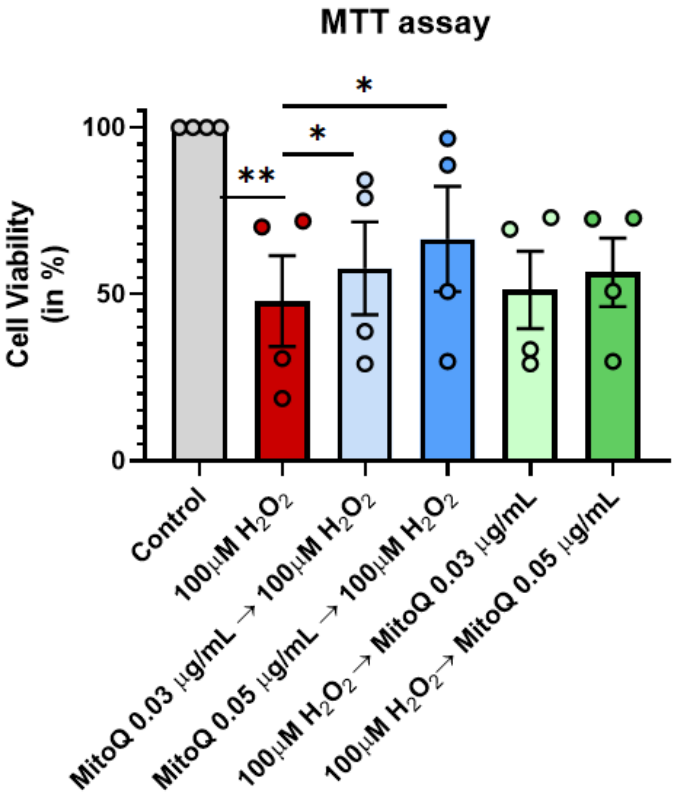


Figure 8 Cell viability measurement by MTT assay.

Values obtained from 4 independent experiments (performed in triplicates) are expressed as percentages normalized to the control. Values are described as mean ± S.E.M. Statistics: ANOVA with Welch's Multiple Comparison post hoc test: *p < 0.05, **p < 0.01,***p < 0.001.

Moreover, the data obtained from the SRB assay (figure 9) reveals a significant decrease in cell growth inhibition from 51% to 35% inhibition when the cells were pre-treated with 0.03 µg/mL MitoQ and from 51% to 33% inhibition when pre-treated with 0.05 µg/mL MitoQ. Such improvement was not to be seen in the post-treated cells.

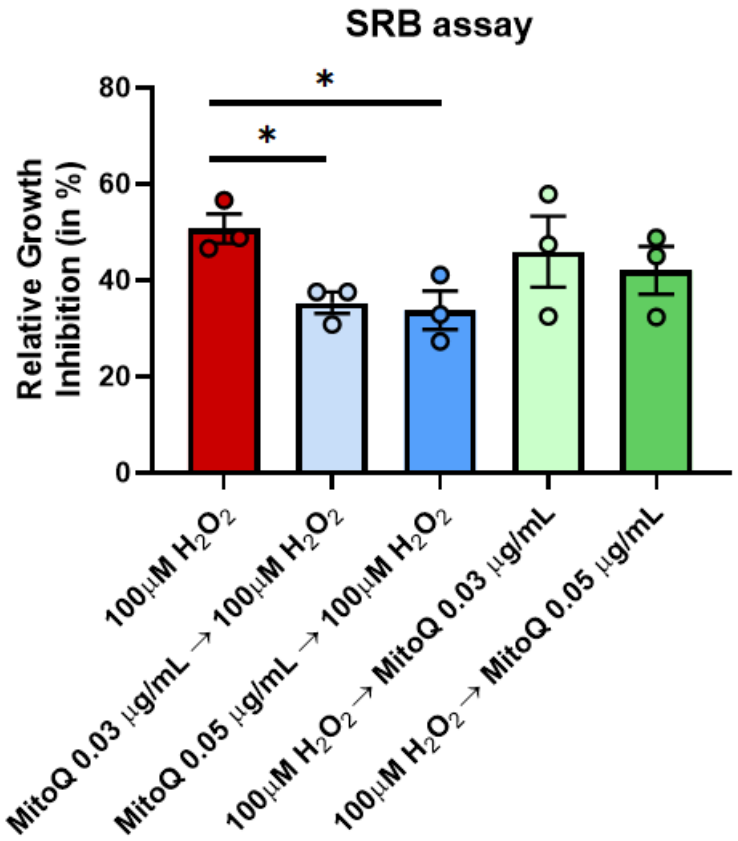


Figure 9 Cell growth inhibition measurement by SRB assay.

Values obtained from 3 independent experiments (performed in triplicates) are expressed as percentages normalized to the control. Values are described as mean ± S.E.M. Statistics: ANOVA with Welch's Multiple Comparison post hoc test: *p < 0.05, **p < 0.01,***p < 0.001.

### 3.2. Pre-treatment with MitoQ helps preserve cell morphology and integrity

The results obtained from both MTT and SRB performed assays are also confirmed by the photomicrographs of SH-SY5Y cells that were taken using phase-contrast microscope (Leica microscope).

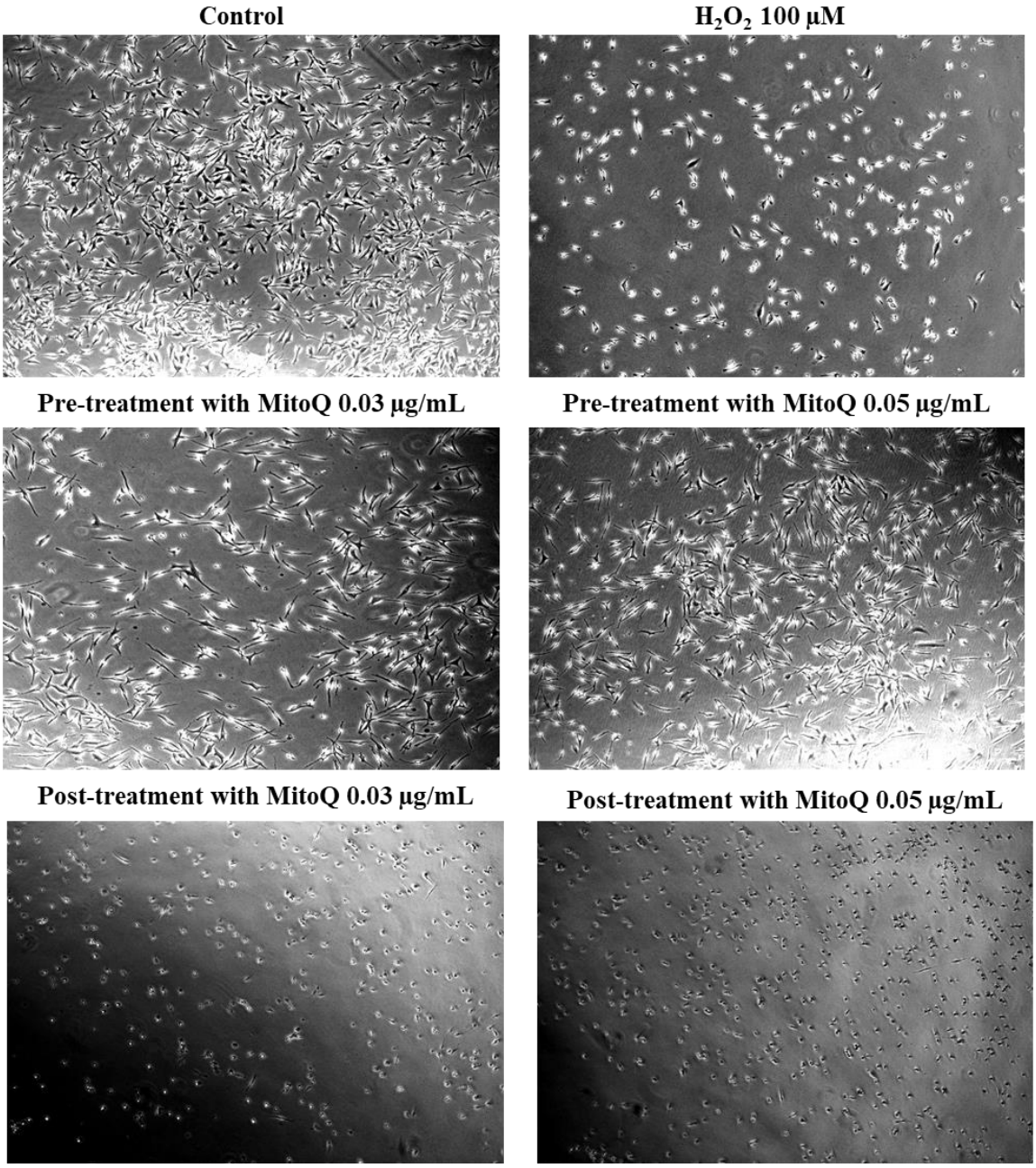


Figure 10 Phase-contrast micrographs taken at 20X magnification

SH-SY5Y morphology and density both seem to be altered by the different treatments.

The $H_2O_2$ only-treated cells (figure 10B) exhibited cell shrinkage accompanied by a reduced number of viable adherent cells compared to the control group (figure 10A) where the elongated epithelial-shaped cells are at high confluency, forming clumps.

However, MitoQ pre-treatment of the neuroblastoma cells seems to protect them from $H_2O_2$ damage with an increased number of adherent and elongated cells (figures 10C and 10D) when compared to the $H_2O_2$ treated group alone (figure 10B). No improvement appears to exist in neither of the post-treatment conditions (figures 10E and 10F).

To further support the cell morphology changes, specific aspect morphology descriptors of the tubulin-stained-cytoskeleton (figures 11A-11D) including roundness and aspect ratio were calculated in order to assess cell shape change in pre-treated cells.

Pre-treatment significantly decreased cell roundness from 0.47 AU to 0.26 AU and 0.32 AU (figure 12A) for the lower and higher concentration of MitoQ respectively while it improved the aspect ratio compared to the $H_2O_2$-treated cells (figure 12B). Such results reflect the protective effect that pre-treatment with MitoQ has on cell morphology and integrity.

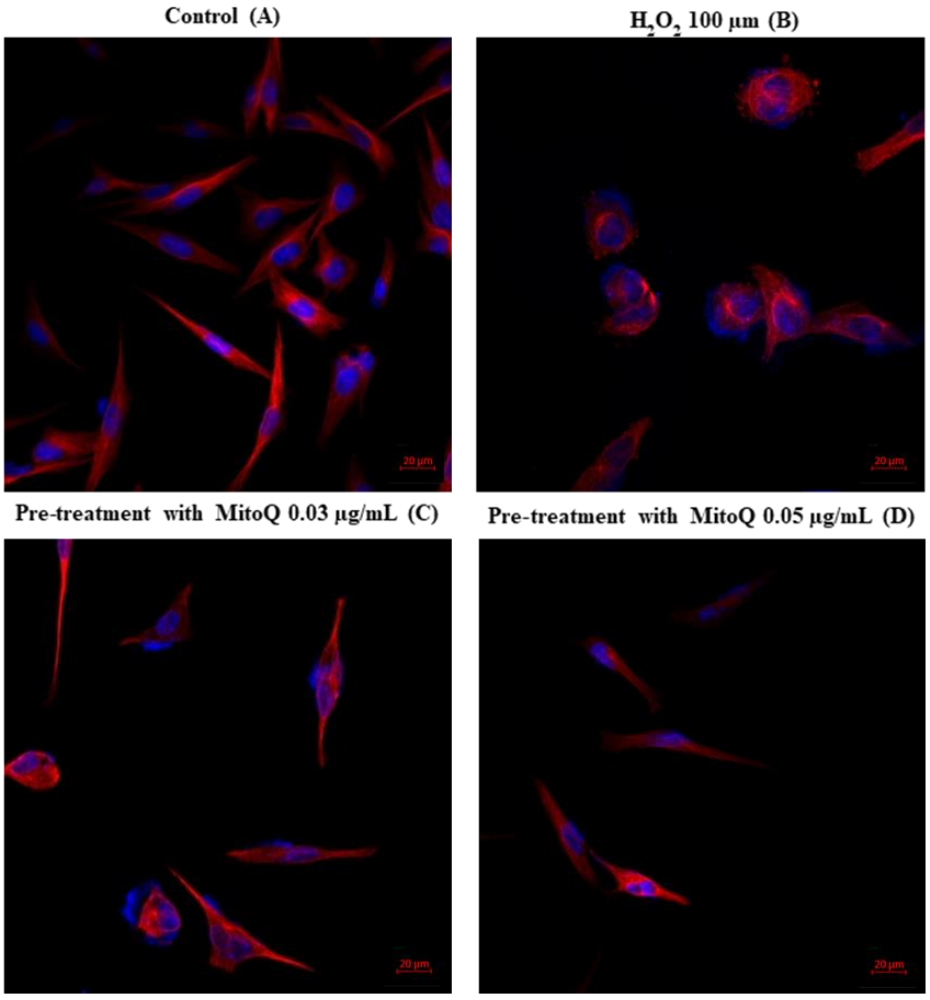


Figure 11 Representative images of β-III tubulin and DAPI co-stain.

The images were taken at 40X oil as Z-stacks with β-III tubulin seen in red and nuclear DAPI stain seen in blue.

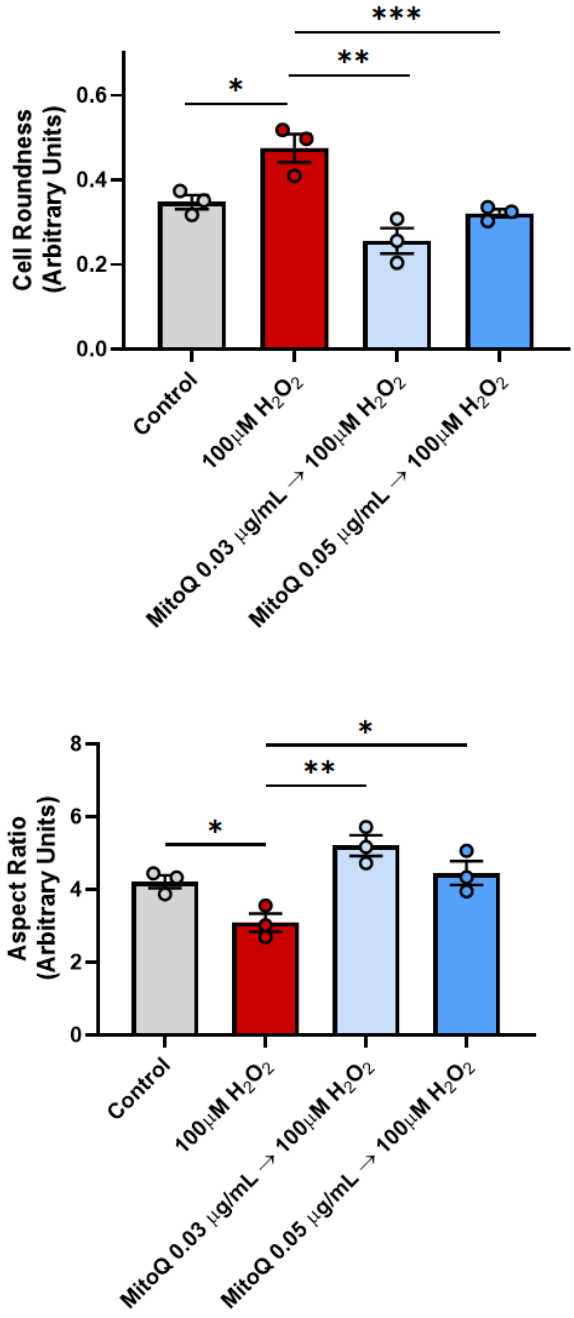


Figure 12 Cell morphology assessment using immunofluorescence images of βIII tubulin.

Two shape descriptors on a per-cell basis were obtained using ImageJ software: cell roundness (upper) and aspect ratio (lower).
Values obtained from 3 experiments are described as mean ± S.E.M.
Statistics: ANOVA with Dunnet's Multiple Comparison post hoc test: *$p < 0.05$, **$p < 0.01$,***$p < 0.001$.

### 3.3. The effect of MitoQ treatment on cell cycle

To better understand the protective mechanism of MitoQ on cell proliferation, the effect of both pre- and post-treatments was investigated using propidium iodide stain.

$H_2O_2$-treatment alone induced a significant increase in SubG0 phase from 27.2% to 66.2% compared to the control group while a significant decrease in G0-G1 phase was calculated (figures 13A and 13B). The latter decrease is significantly attenuated by the pre-treatment with MitoQ at 0.03 µg/mL and 0.05 µg/mL, the percentage of cells in G0-G1 arrest increasing from 14.7 % to 29.3% and 30.7% respectively (figures 13B – 13F).

Moreover, pre-treatment with MitoQ at both concentrations significantly increased the percentage of cells in S phase from 4.6% to 6.9% at the lower concentration and 7.5% at the higher concentration (figures 13B-13G).

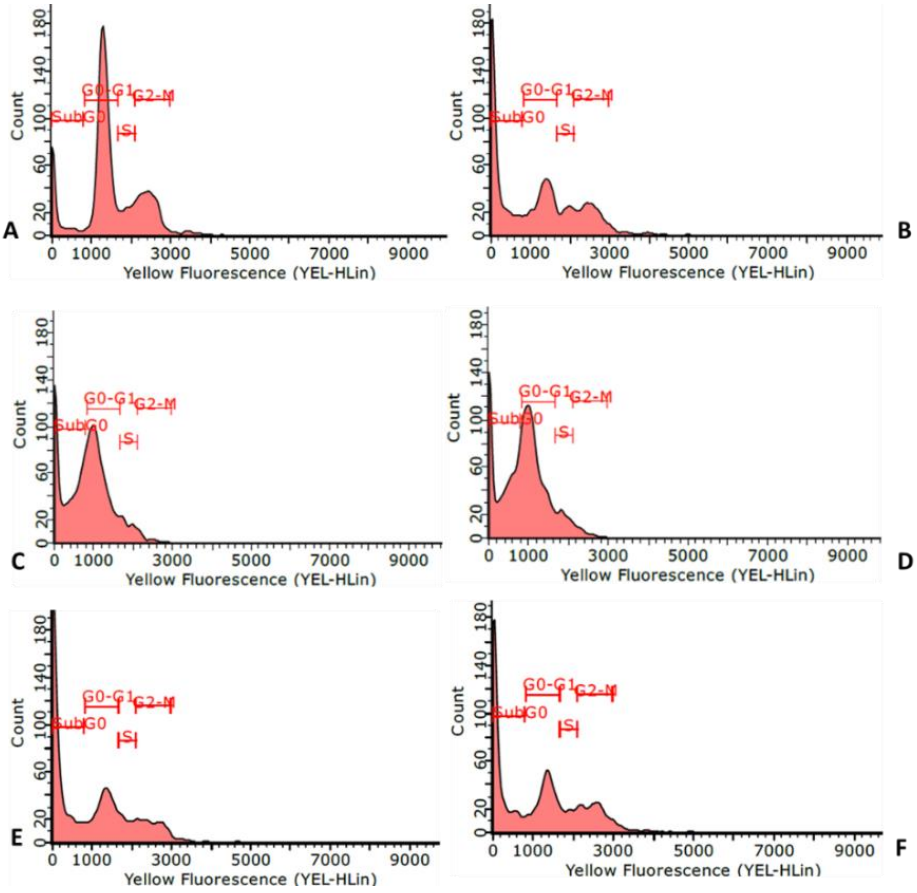

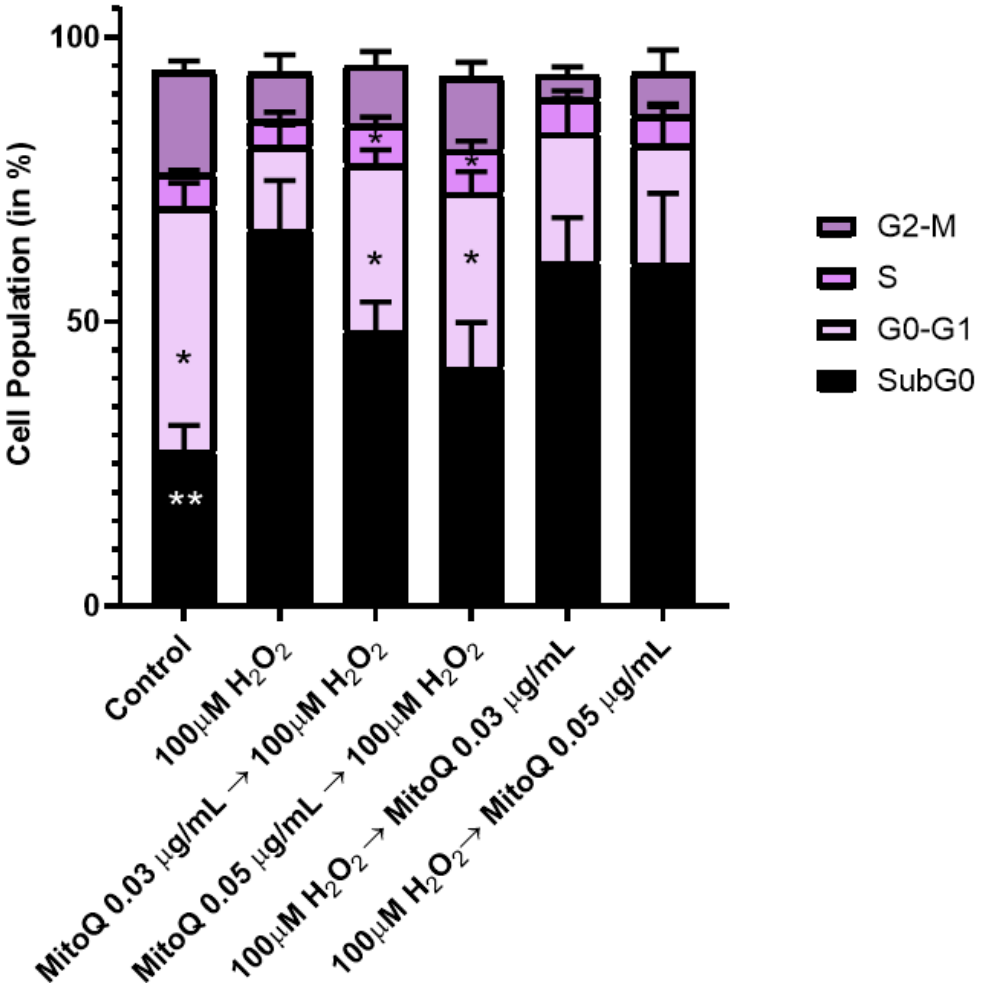


Figure 13 Cell cycle analysis of SH-SY5Y cells.

Cell distribution in the different cell cycle phases by the different treatments.
A: Control; B: 100μM $H_2O_2$; C: pre-treatment with MitoQ 0.03 μg/mL; D: pre-treatment with MitoQ 0.05 μg/mL; E: post-treatment with MitoQ 0.03 μg/mL; F: post-treatment with MitoQ 0. 05 μg/mL.
Values obtained from 4 experiments are described as mean ± S.E.M. Statistics: ANOVA with Dunnet's Multiple Comparison post hoc test: *$p < 0.05$, **$p < 0.01$,***$p < 0.001$.

### 3.4. MitoQ treatment ameliorates oxidative stress levels

The levels of ROS generated by the neuroblastoma cells were obtained using the fluorescent probe DHE which will emit an intense red color following its oxidation in the presence of reactive species.

As shown in figure 14, $H_2O_2$ treatment resulted in a significant increase in ROS generation which was revealed by the increased DHE intensity compared to the control group (figures 14A and 14B).

Meanwhile, pre-treatment of SH-SY5Y cells with MitoQ attenuated and reversed the increase in $H_2O_2$-induced ROS generation with a significant decrease in DHE intensity from 1.16-fold change to 0.67- and 0.55-fold change respectively when 0.03 µg/mL and 0.05 µg/mL of MitoQ were added for 24 hours prior the $H_2O_2$-induction of neurotoxicity (figures 14B-14D).

Similarly, post-treatment with 0.03 µg/mL MitoQ significantly decreased the intensity of the signal (figure 14E). However, no significant change was obtained when MitoQ was used at the higher concentration on the already $H_2O_2$-stressed cells (figure 14F).

Moreover, the NBT assay data comes to support the finding that pre-treatment with MitoQ does indeed improve oxidative stress. In fact, pre-treating SH-SY5Y cells with 0.03 µg/mL or 0.05 µg/mL of MitoQ produced significantly lesser ROS amount (33.4% and 23.1% respectively) compared to the $H_2O_2$-only treated cells characterized by a high percentage of ROS production (52.8%). However, post-treatment does not seem to effectively improve oxidative stress (figure 15).

Control (A)

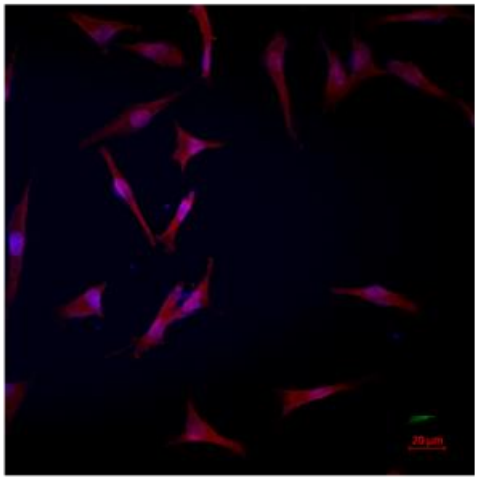

$H_2O_2$ 100 µM (B)

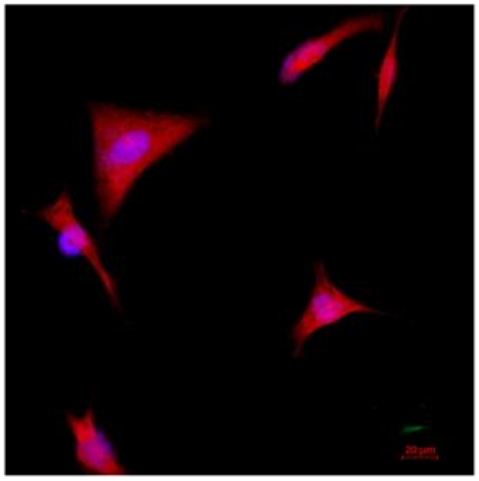

Pre-treatment with MitoQ 0.03 µg/mL (C)

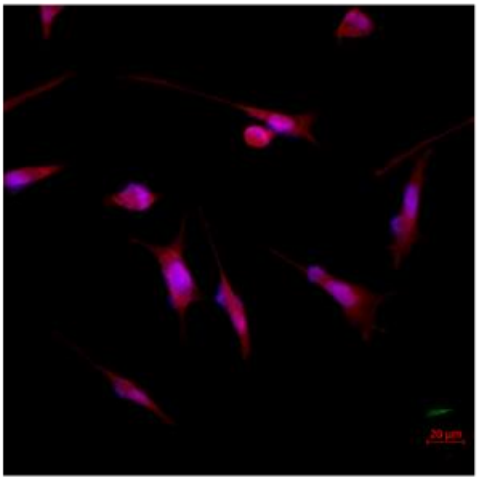

Pre-treatment with MitoQ 0.05 µg/mL (D)

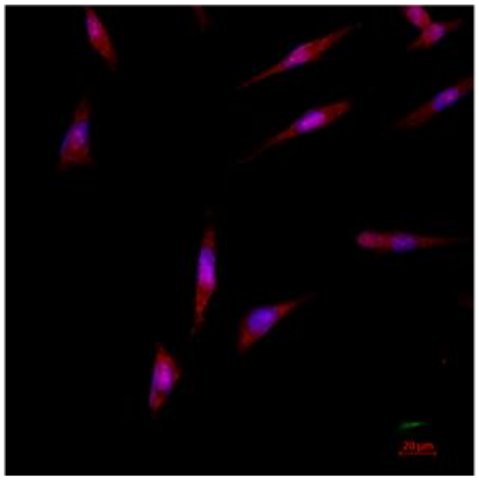

Post-treatment with MitoQ 0.03 µg/mL (E)

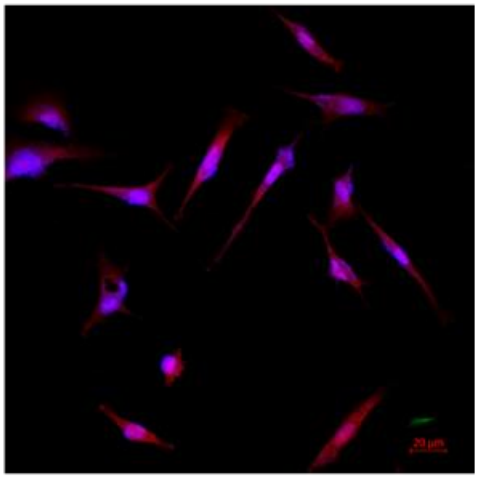

Post-treatment with MitoQ 0.05 µg/mL (F)

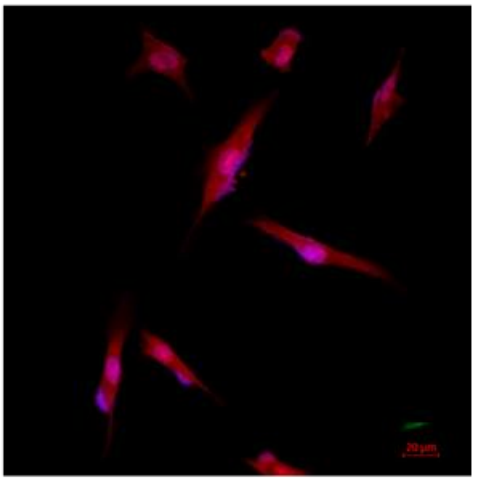

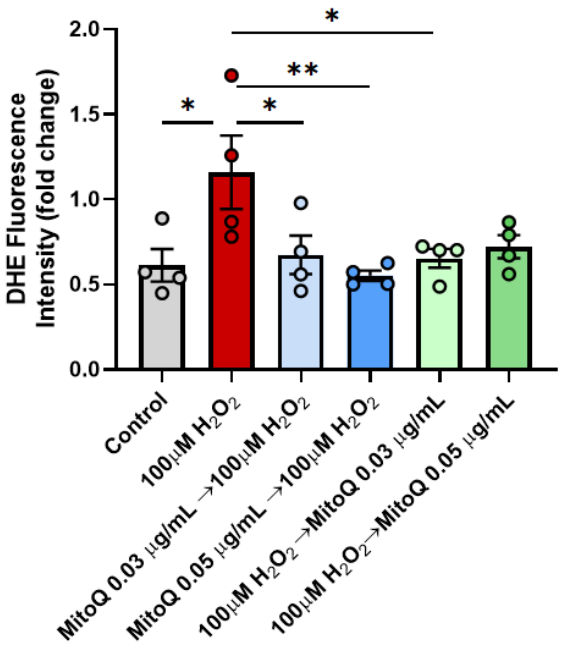


Figure 14 (A-F) Representative images of DHE and DAPI co-staining.

Oxidative stress assessment by DHE intensity analysis.

The images were taken at 40X oil as Z-stacks; DHE seen in red and nuclear DAPI stain seen in blue.

Values obtained from 4 experiments (performed in quadruplicates) are expressed as fold change in intensity are described as mean ± S.E.M.
Statistics: ANOVA with Welch's Multiple Comparison post hoc test: *p < 0.05, **p < 0.01,***p < 0.001.

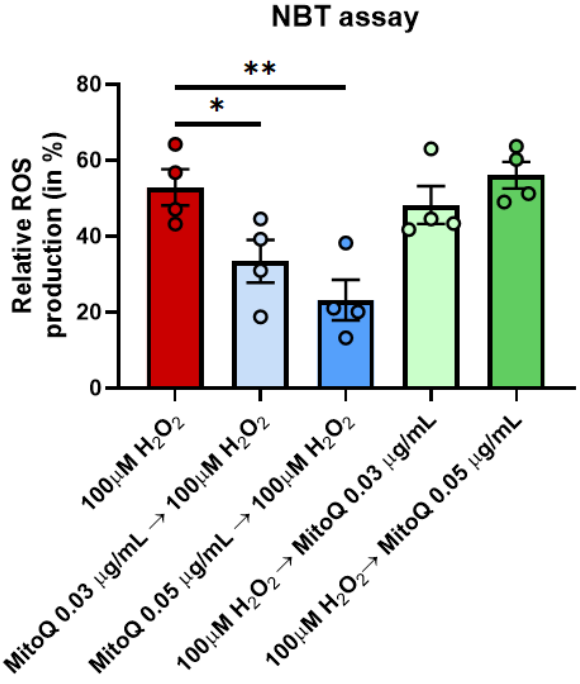


Figure 15 ROS levels measurement by NBT reduction assay.
Values obtained from 4 independent experiments (performed in triplicates) are described as mean ± S.E.M.
Statistics: ANOVA with Welch's Multiple Comparison post hoc test: *p < 0.05, **p < 0.01, ***p < 0.001.

### 3.5. MitoQ treatment protects the mitochondrial phenotype

MitotrackerGreen staining was used to investigate the changes in mitochondrial morphology that the different treatments induced by computing two main shape descriptors on a per-cell basis: cell circularity and aspect ratio.

**Control (A)**

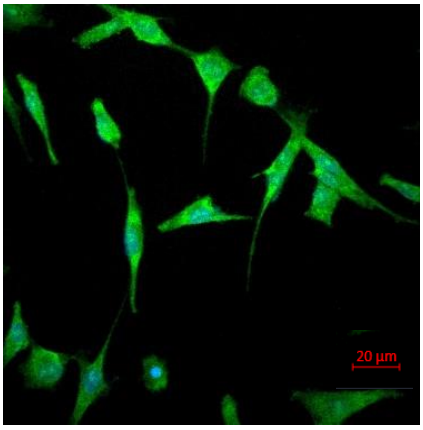


**$H_2O_2$ 100 µM (B)**

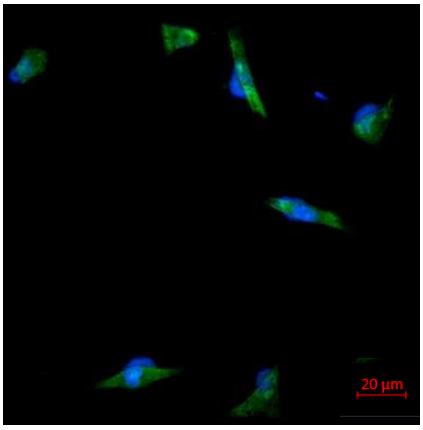


**Pre-treatment with MitoQ 0.03 µg/mL (C)**

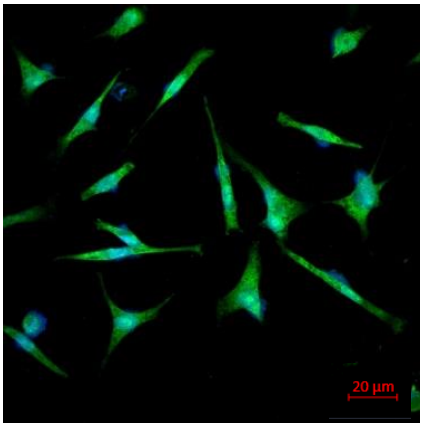


**Pre-treatment with MitoQ 0.05 µg/mL (D)**

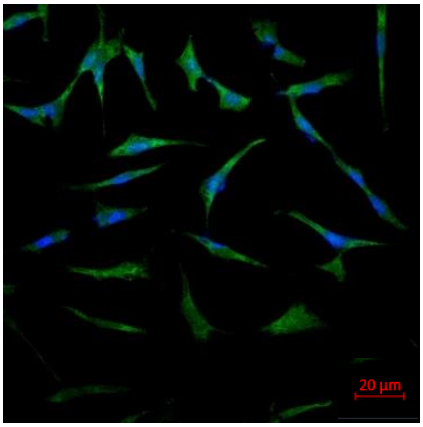


**Post-treatment with MitoQ 0.03 µg/mL (E)**

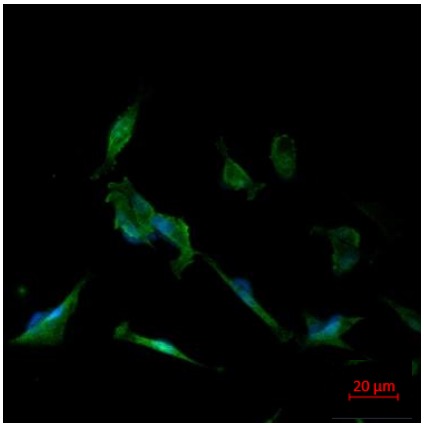


**Post-treatment with MitoQ 0.05 µg/mL (F)**

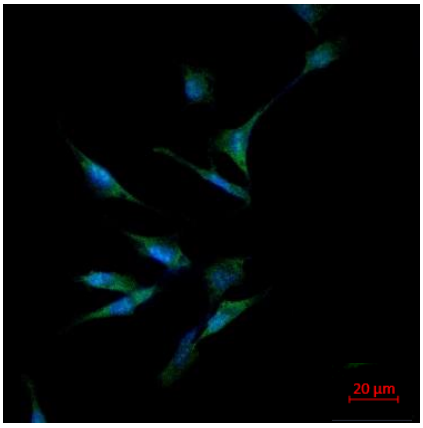

Figure 16 (A-F) Representative images of MitotrackerGreen and DAPI stain.
The images were taken at 40X oil as Z-stacks; mitochondrial content seen in green and nuclear DAPI stain seen in blue

Following $H_2O_2$ treatment for 24 hours, the characteristic elongated form of the mitochondria shifts to a shortened, rounded appearance (figures 16A and 16C). However, pre-treating SH-SY5Y cells with either low or high concentration of MitoQ helps in conserving the mitochondria's characteristics which is revealed by the significant decrease in mitochondrial circularity from 0.54 AU to 0.40 AU and 0.30 AU respectively (figure 17).

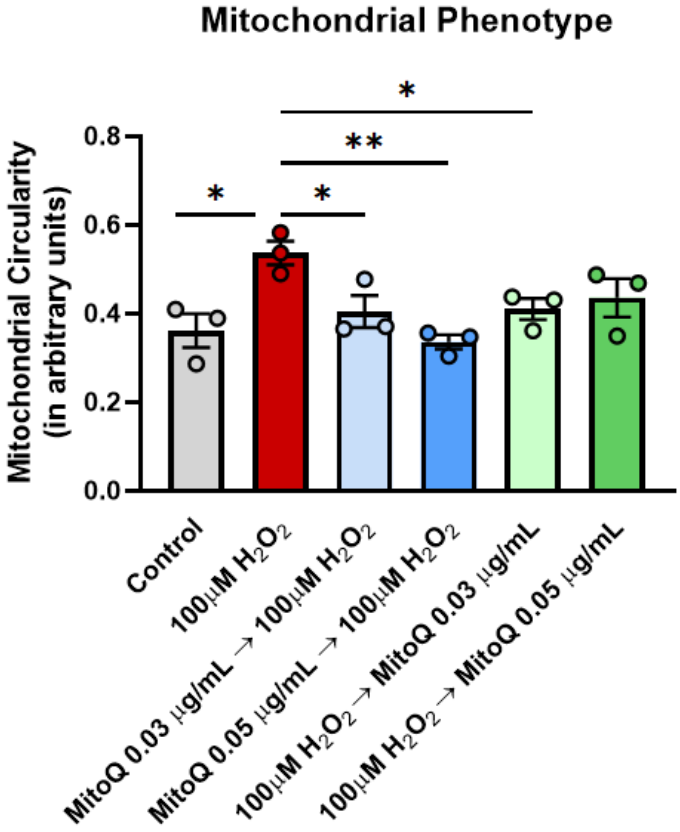


Figure 17 Mitochondrial circularity assessment.

Values obtained from 3 experiments are described as mean ± S.E.M.
Statistics: ANOVA with Dunnet's Multiple Comparison post hoc test: *p < 0.05, **p < 0.01,***p < 0.001.

Moreover, cells pre-treated with 0.03 µg/mL or 0.05 µg/mL MitoQ had a higher aspect ratio of the organelle, 3.97 AU (figures 16C and 18) and 4.26 AU (figures 16D and 18) respectively, compared to the $H_2O_2$-only treated cells which were characterized by a low aspect ratio value of 2.52 AU (figure 18).

.

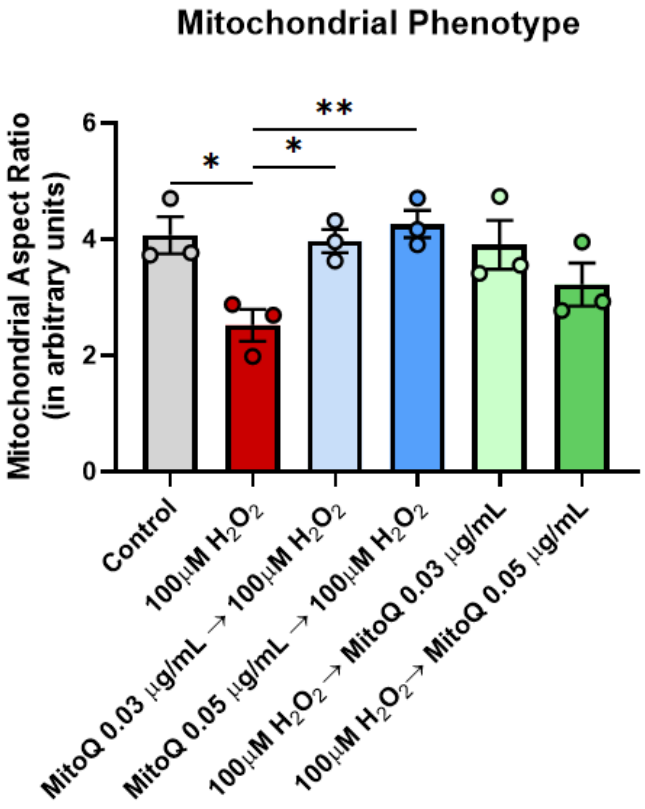


Figure 18 Mitochondrial aspect ratio assessment.

Values obtained from 3 experiments are described as mean ± S.E.M.
Statistics: ANOVA with Dunnet's Multiple Comparison post hoc test: *p < 0.05, **p < 0.01,***p < 0.001.

### 3.6. The involvement of the Nrf2 pathway in the protective effect of MitoQ

To investigate the effect of MitoQ on the Nrf2-Keap-ARE signaling pathway, relative mRNA levels of Nrf2 were obtained by RT-qPCR.

The results showed that, when treated for 24 hours with $H_2O_2$ only, a significant decrease in Nrf2 gene expression was noted, from a 2.29- to a 1.04- fold change. This decrease is significantly lessened when the cells are pre-treated with MitoQ, with values going back to control levels (2.52- and 2.54- fold change) (figure 19).

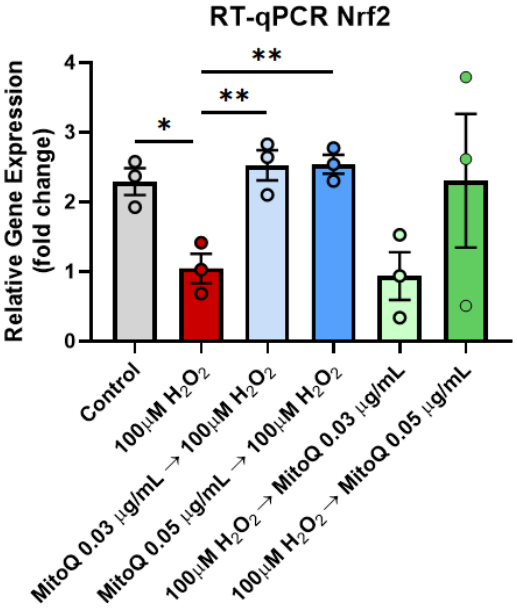


Figure 19 Evaluation by RT-qPCR of the mRNA levels of the transcription factor Nrf2 expressed as fold change.

Values obtained from 3 experiments are described as mean ± S.E.M. Statistics: ANOVA with Welch's Multiple Comparison post hoc test. *p < 0.05, **p < 0.01,***p < 0.001.

However, when studying Nrf2 protein levels in the differently treated cells via immunofluorescence imaging, opposing results were to be observed. Stress induction by $H_2O_2$ treatment induced upregulation in protein expression observed as a greater immunocytochemistry signal of 0.32-fold change compared to the untreated cells with a signal intensity of 0.17-fold change. However, MitoQ treatment prior to that of $H_2O_2$

hindered this increase with signal intensity significantly decreasing to 0.22-fold change at both concentrations (figures 20 B-D).

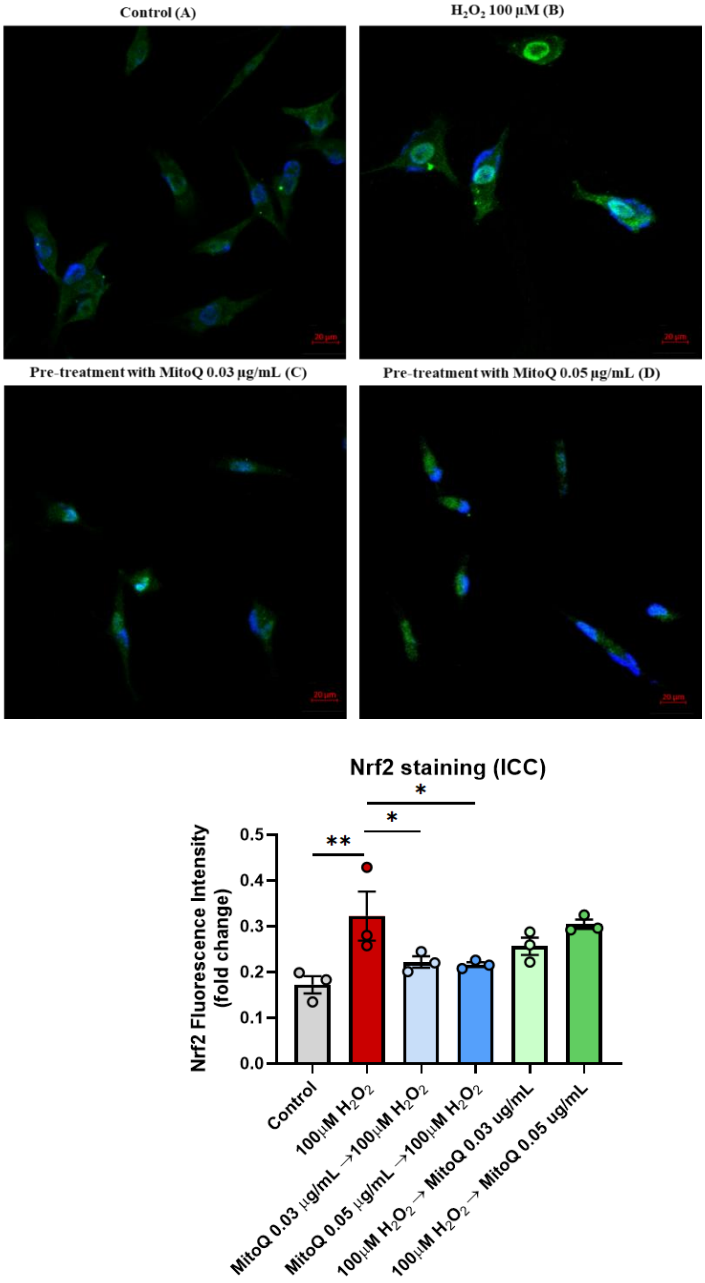


Figure 20 (A-D) Representative images of Nrf2 and DAPI co-staining. Protein expression of Nrf2 assessment by signal intensity analysis.

The images were taken at 40X oil as Z-stacks; Nrf2 seen in green and nuclear DAPI stain seen in blue.

Values obtained from 3 experiments are described as mean ± S.E.M. Statistics: ANOVA with Welch's Multiple Comparison post hoc test. *p < 0.05, **p < 0.01,***p < 0.001.

In order to investigate furthermore the effect of MitoQ treatment on antioxidant activity, the gene expression of three cyto-protective genes which are downstream antioxidant players in the Nrf2-Keap-ARE pathway – SOD1, HOX1 and CAT - was examined by RT-qPCR.

The results reveal that pre-treatment with MitoQ at both low and high concentrations significantly decreased the mRNA level of SOD1 to 0.62 and 1.00-fold change respectively compared to the $H_2O_2$ only-treated cells characterized by a high gene expression of 2.60-fold change. However, only post-treatment with 0.03 µg/mL of MitoQ led to a similar significant decrease in SOD1 expression while no effect was to be recorded in post-treatment with 0.05 µg/mL (figure 21).

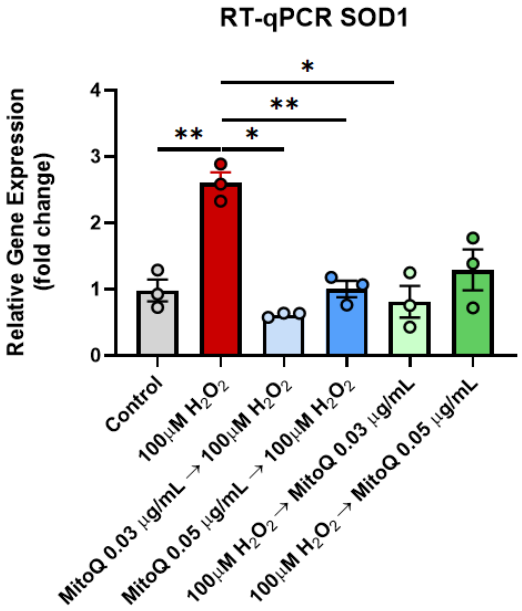


Figure 21 Evaluation by RT-qPCR of the mRNA levels of the antioxidant gene superoxide dismutase 1 expressed as fold change.

Values obtained from 3 experiments are described as mean ± S.E.M.
Statistics: ANOVA with Welch's Multiple Comparison post hoc test. *p < 0.05, **p < 0.01,***p < 0.001.

Moreover, treating SH-SY5Y cells with MitoQ prior to $H_2O_2$ induction of stress seems to limit the decrease in HOX1 gene expression that results from $H_2O_2$ treatment. In fact, an increase in mRNA levels of this antioxidant gene from 0.56-fold change to 1.62- and 1.15-fold change in cells pre-treated with MitoQ 0.03 µg/mL and MitoQ 0.05 µg/mL is noted (figure 22).

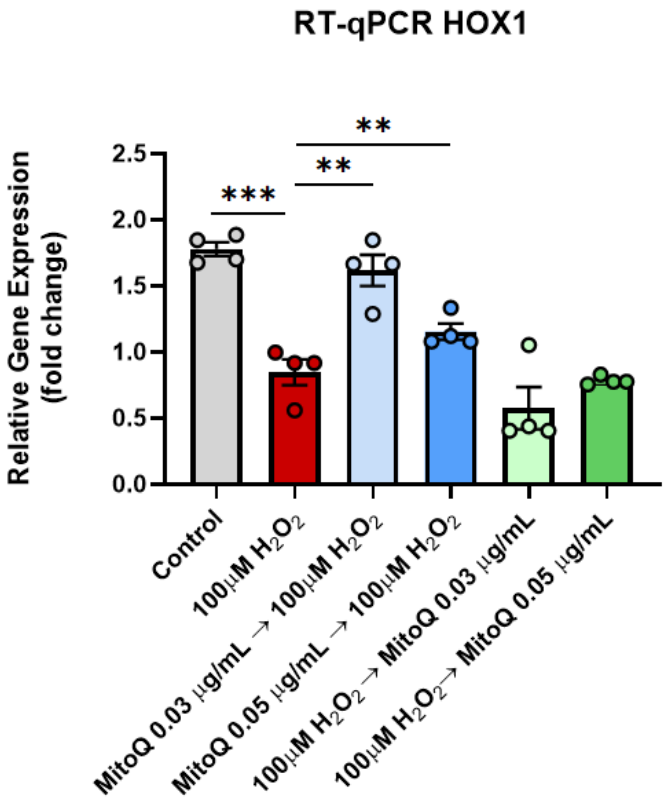


Figure 22 Evaluation by RT-qPCR of the mRNA levels of the antioxidant gene heme oxygenase 1 expressed as fold change.

Values obtained from 4 experiments are described as mean ± S.E.M.
Statistics: ANOVA with Welch's Multiple Comparison post hoc test. *p < 0.05, **p < 0.01,***p < 0.001

However, no significant change in CAT mRNA levels was noted in neither pre- nor post-treatment conditions suggesting that MitoQ does not affect CAT activity (figure 23).

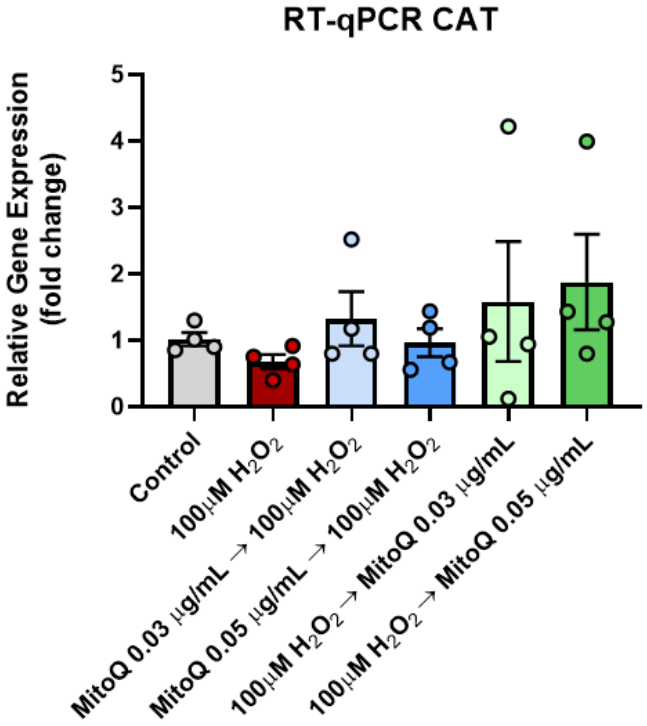


Figure 23 Evaluation by RT-qPCR of the mRNA levels of the antioxidant gene catalase expressed in fold change.

Values obtained from 4 experiments are described as mean ± S.E.M.
Statistics: ANOVA with Welch's Multiple Comparison post hoc test. *p < 0.05, **p < 0.01,***p < 0.001.

### 3.6. Pre-treatment with MitoQ reduces inflammation

Cyclooxygenase-2 (COX-2) is one enzyme that majorly contributes to inflammatory processes following its induced expression by oxidative stress.

Mimicking neurotoxicity via treatment of SH-SY5Y cells with $H_2O_2$ led to a significant increase in mRNA levels of COX-2 to a 3.83-fold change compared to the control cells characterized by a low fold change of 0.77 (figure 24).

However, treating the cells with 0.05 µg/mL MitoQ prior to $H_2O_2$ treatment improved inflammation by significantly decreasing COX-2 mRNA levels to 1.56-foldchange (figure 24).

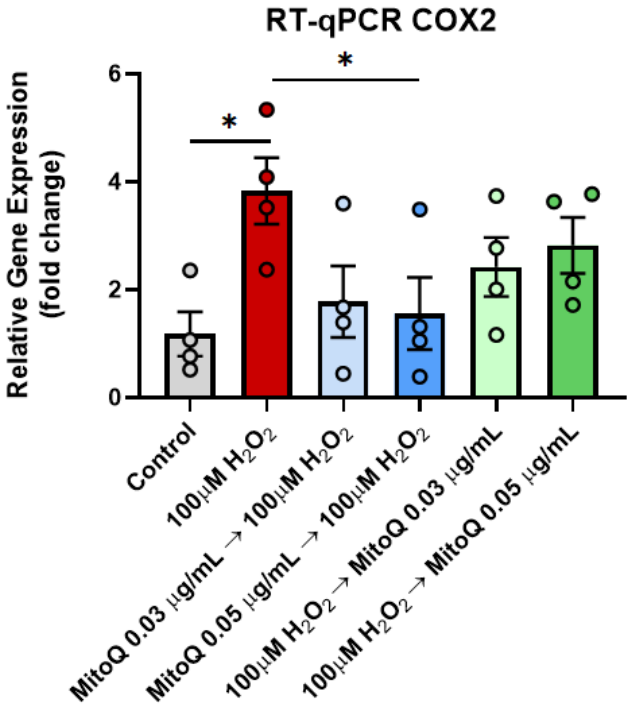


Figure 24 Evaluation by RT-qPCR of the mRNA levels of the pro-inflammatory gene COX-2 expressed in fold change.

Values obtained from 4 experiments are described as mean ± S.E.M. Statistics: ANOVA with Welch's Multiple Comparison post hoc test. *p < 0.05, **p < 0.01,***p < 0.001.

In addition, even though no significant change was obtained in the expression of NFκB - a central mediator of inflammation that is crucial in TBI pathogenesis – when administered as a pre-treatment, the antioxidant does seem to cause a decrease in the protein levels at both concentrations when compared to the $H_2O_2$-treated cells only (figure 25).

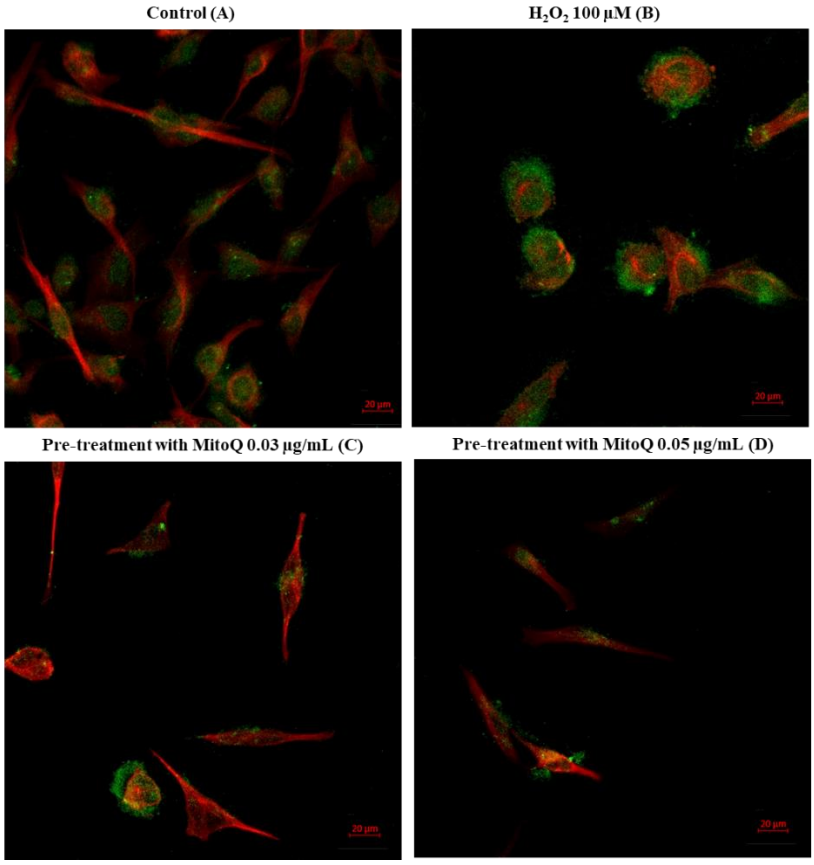


Figure 25 Representative images of NFκB and tubulin co-staining.

The images were taken at 40X oil as Z-stacks; NFκB stain seen in green and tubulin seen in red.

Values obtained from 3 experiments are expressed as fold change in intensity and are described as mean ± S.E.M.
Statistics: ANOVA with Welch's Multiple Comparison post hoc test: *p < 0.05, **p < 0.01,***p < 0.001.

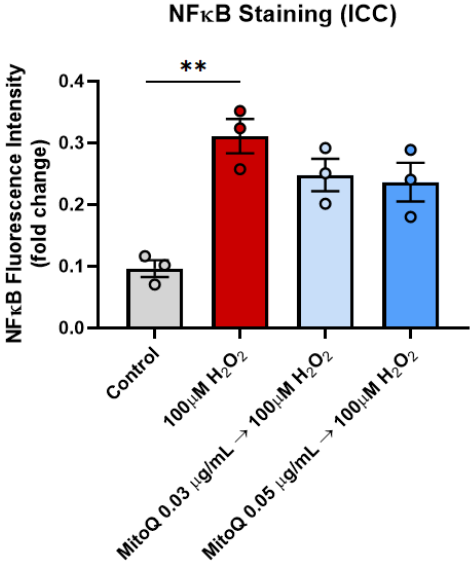

# CHAPTER 5

# DISCUSSION

The current study demonstrated that the mitochondrial-target antioxidant MitoQ exerts significant neuroprotective effects against $H_2O_2$-induced neurotoxicity when used as a pre-treatment by increasing cell viability, preserving cell morphology and cell cycle integrity in SH-SY5Y cells.

Moreover, pre-treatment with MitoQ limited oxidative stress generation while protecting mitochondria from extensive damage by conserving its characteristic phenotype.

The protective effectives resulting from pre-treatment with MitoQ seems to stem from its interaction with the Nrf2-Keap-ARE pathway, a major player in oxidative stress. In fact, gene expression of the transcription factor itself as well as its main downstream cytoprotective and antioxidant enzyme HMOX1 are increased and closer to normal values when cells are pre-treated with MitoQ.

The opposing Nrf2 data obtained from RT-qPCR and ICC could be explained by the temporal delay in the correlation of mRNA and protein expression (Guo et al., 2008). Another explanation could be the nuclear localization/activation of Nrf2 observed in the $H_2O_2$-only treated group: the strong nuclear intensity resulting from localization might be responsible for the elevated value of Nrf2 protein expression even though cytosolically, the signal intensity is lower compared to the control which parallels the mRNA data across all conditions.

Moreover, the increase in mRNA SOD1 levels following stress induction which was attenuated by MitoQ pre-treatment makes sense considering that the cytosolic copper-containing enzyme is responsible for neutralizing the harmful superoxide free

radicals produced by the mitochondria via dismutation of superoxide into oxygen and $H_2O_2$ (Juarez et al., 2008; Vu et al., 2012).

All those findings, added to the widely studied anti-inflammatory effect that MitoQ exerts both *in vivo* and *in vitro* (Piscianz et al., 2021) which is here observed by the change in COX-2 expression across the different treatments of SH-SY5Y cells, come to support the use of this mitochondrial-targeted antioxidant to protect neuronal-like cells from oxidative stress and damage, the main aspect of secondary brain injury.

As previously stated in the introduction, the central nervous system (CNS) is very sensitive to oxidation, making it most vulnerable to oxidative stress damage and hence neurodegeneration. For that reason, targeting antioxidant activity is crucial as a therapeutic approach to lessen and reduce neuronal damage resulting from ROS accumulation, a common and recurrent aspect of many brain diseases. And because the respiratory organelle is the main producer of cellular ROS, mitochondria-targeted antioxidants that are readily available and that would selectively accumulate in the cell's powerhouse would provide the most encouraging neuroprotective effects.

MitoQ is one of those promising antioxidants that is being studied more and more these past few years. It is characterized by a good uptake by cells in culture which permits the rapid equilibration of MitoQ across the plasma membrane potential leading to its accumulation into the mitochondria (Kelso et al., 2001). For that, MitoQ has been studied *in vitro* in a large number of cell models of mitochondrial oxidative stress where it has shown protection against ROS-induced damage (Apostolova et al., 2011; Jauslin, Meier, Smith, & Murphy, 2003; Zhong et al., 2021) similar to the results obtained on SH-SY5Y cells from this study.

Moreover, research over the years revealed that Nrf2 is the key regulator in reducing oxidative stress, inflammatory response, and toxic metabolites accumulation, all three processes being involved in several neurological disorders including but not limited to TBI (Ding et al., 2014; Ma, 2013; Yan, Wang, Hu, Wang, & Yin, 2008). And many studies both *in vitro* and *in vivo* showed that MitoQ up-regulates the expression of several of these downstream pro-survival genes and hence counteracts oxidative damage (Tufekci, Civi Bayin, Genc, & Genc, 2011). In fact, a study from our lab has recently revealed the implication of the Nrf2 pathway in the neuroprotective effects of MitoQ treatment for 30 days in a mouse model of open-head TBI where an increase in the relative expression of all Nrf2, SOD and CAT genes was noted (Haidar et al., 2022). Moreover, an *in vitro* study by Zhu et al. showed that the knockdown of Nrf2 significantly abolishes the protective effects of MitoQ (Z. Zhu et al., 2021). The latter, along with our results showing expression change in Nrf2, SOD1 and HOX1, suggest that Nrf2 signaling is majorly involved in the protection of MitoQ against $H_2O_2$-induced neurotoxicity.

A lot still needs to be investigated in order to fully explain the mechanisms by which pre-treatment with MitoQ protects SH-SY5Y cells from $H_2O_2$-induced neurotoxicity. In fact, a broader and deeper investigation of the effect that MitoQ has on inflammatory processes would allow us to have a better understanding of its anti-inflammatory properties. Also, supporting the RT-qPCR data that revealed the effect that MitoQ has on certain anti-oxidant with immunoblotting is to be considered.

Moreover, repeating all the experiments on another cell-line similar to SH-SY5Y cells (such as neuroblastoma PC-12 cells) or even on primary neuronal cells is needed to confirm that the protective effect of MitoQ is not just specific to the cell line used.

Inducing neurotoxicity by using another chemical and checking if the protective role of MitoQ is preserved would further support the effectiveness of the treatment.

Lastly, because the chosen antioxidant is mitochondria-targeted, additional experiments that would further study the effect that MitoQ has on mitochondria such as mitochondrial mass content determination and mitochondrial membrane potential disruption/maintenance are still to be conducted.

Studying the effect that MitoQ has on respiration by measuring oxygen consumption or looking for any change in the activity of the different mitochondrial complexes would add more to the findings and would allow us to fully understand how neuroprotection is attained by MitoQ treatment.

# REFERENCES


Apostolova, N., Garcia-Bou, R., Hernandez-Mijares, A., Herance, R., Rocha, M., & Victor, V. M. (2011). Mitochondrial antioxidants alleviate oxidative and nitrosative stress in a cellular model of sepsis. *Pharm Res, 28*(11), 2910-2919. doi:10.1007/s11095-011-0528-0

Aruoma, O. I., & Halliwell, B. (1987). Superoxide-dependent and ascorbate-dependent formation of hydroxyl radicals from hydrogen peroxide in the presence of iron. Are lactoferrin and transferrin promoters of hydroxyl-radical generation? *Biochem J, 241*(1), 273-278. doi:10.1042/bj2410273

Borgens, R. B., & Liu-Snyder, P. (2012). Understanding secondary injury. *Q Rev Biol, 87*(2), 89-127. doi:10.1086/665457

Capizzi, A., Woo, J., & Verduzco-Gutierrez, M. (2020). Traumatic Brain Injury: An Overview of Epidemiology, Pathophysiology, and Medical Management. *Med Clin North Am, 104*(2), 213-238. doi:10.1016/j.mcna.2019.11.001

Cen, M., Ouyang, W., Zhang, W., Yang, L., Lin, X., Dai, M., . . . Xu, F. (2021). MitoQ protects against hyperpermeability of endothelium barrier in acute lung injury via a Nrf2-dependent mechanism. *Redox Biol, 41*, 101936. doi:10.1016/j.redox.2021.101936

Choi, H. S., Kim, J. W., Cha, Y. N., & Kim, C. (2006). A quantitative nitroblue tetrazolium assay for determining intracellular superoxide anion production in phagocytic cells. *J Immunoassay Immunochem, 27*(1), 31-44. doi:10.1080/15321810500403722

D'Autreaux, B., & Toledano, M. B. (2007). ROS as signalling molecules: mechanisms that generate specificity in ROS homeostasis. *Nat Rev Mol Cell Biol, 8*(10), 813-824. doi:10.1038/nrm2256

Datla, S. R., & Griendling, K. K. (2010). Reactive oxygen species, NADPH oxidases, and hypertension. *Hypertension, 56*(3), 325-330. doi:10.1161/HYPERTENSIONAHA.109.142422

Davis, C. K., & Vemuganti, R. (2022). Antioxidant therapies in traumatic brain injury. *Neurochem Int, 152*, 105255. doi:10.1016/j.neuint.2021.105255

Devi, Y., Khan, S., Rana, P., Deepak, Dhandapani, M., Ghai, S., . . . Dhandapani, S. (2020). Cognitive, Behavioral, and Functional Impairments among Traumatic Brain Injury Survivors: Impact on Caregiver Burden. *J Neurosci Rural Pract, 11*(4), 629-635. doi:10.1055/s-0040-1716777

Dewan, M. C., Rattani, A., Gupta, S., Baticulon, R. E., Hung, Y. C., Punchak, M., . . . Park, K. B. (2018). Estimating the global incidence of traumatic brain injury. *J Neurosurg*, 1-18. doi:10.3171/2017.10.JNS17352

Dikmen, S. S., Corrigan, J. D., Levin, H. S., Machamer, J., Stiers, W., & Weisskopf, M. G. (2009). Cognitive outcome following traumatic brain injury. *J Head Trauma Rehabil, 24*(6), 430-438. doi:10.1097/HTR.0b013e3181c133e9

Ding, K., Wang, H., Xu, J., Li, T., Zhang, L., Ding, Y., . . . Zhou, M. (2014). Melatonin stimulates antioxidant enzymes and reduces oxidative stress in experimental traumatic brain injury: the Nrf2-ARE signaling pathway as a potential mechanism. *Free Radic Biol Med, 73*, 1-11. doi:10.1016/j.freeradbiomed.2014.04.031

Elsayed Azab, A., A Adwas, A., Ibrahim Elsayed, A. S., A Adwas, A., Ibrahim Elsayed, A. S., & Quwaydir, F. A. (2019). Oxidative stress and antioxidant mechanisms in human body. *Journal of Applied Biotechnology & Bioengineering, 6*(1), 43-47. doi:10.15406/jabb.2019.06.00173

Fann, J. R., Katon, W. J., Uomoto, J. M., & Esselman, P. C. (1995). Psychiatric disorders and functional disability in outpatients with traumatic brain injuries. *Am J Psychiatry, 152*(10), 1493-1499. doi:10.1176/ajp.152.10.1493

Forster, J. I., Koglsberger, S., Trefois, C., Boyd, O., Baumuratov, A. S., Buck, L., . . . Antony, P. M. (2016). Characterization of Differentiated SH-SY5Y as Neuronal Screening Model Reveals Increased Oxidative Vulnerability. *J Biomol Screen, 21*(5), 496-509. doi:10.1177/1087057115625190

Fujita, Y., Izawa, Y., Ali, N., Kanematsu, Y., Tsuchiya, K., Hamano, S., . . . Yoshizumi, M. (2006). Pramipexole protects against H2O2-induced PC12 cell death. *Naunyn Schmiedebergs Arch Pharmacol, 372*(4), 257-266. doi:10.1007/s00210-005-0025-2

Greve, M. W., & Zink, B. J. (2009). Pathophysiology of traumatic brain injury. *Mt Sinai J Med, 76*(2), 97-104. doi:10.1002/msj.20104

Guo, Y., Xiao, P., Lei, S., Deng, F., Xiao, G. G., Liu, Y., . . . Deng, H. (2008). How is mRNA expression predictive for protein expression? A correlation study on human circulating monocytes. *Acta Biochim Biophys Sin (Shanghai), 40*(5), 426-436. doi:10.1111/j.1745-7270.2008.00418.x

Haidar, M. A., Shakkour, Z., Barsa, C., Tabet, M., Mekhjian, S., Darwish, H., . . . Kobeissy, F. (2022). Mitoquinone Helps Combat the Neurological, Cognitive,

and Molecular Consequences of Open Head Traumatic Brain Injury at Chronic Time Point. *Biomedicines, 10*(2). doi:10.3390/biomedicines10020250

Halliwell, B., & Gutteridge, J. M. (1984). Oxygen toxicity, oxygen radicals, transition metals and disease. *Biochem J, 219*(1), 1-14. doi:10.1042/bj2190001

Harvey, C. J., Thimmulappa, R. K., Singh, A., Blake, D. J., Ling, G., Wakabayashi, N., . . . Biswal, S. (2009). Nrf2-regulated glutathione recycling independent of biosynthesis is critical for cell survival during oxidative stress. *Free Radic Biol Med, 46*(4), 443-453. doi:10.1016/j.freeradbiomed.2008.10.040

Heusinkveld, H. J., & Westerink, R. H. S. (2017). Comparison of different in vitro cell models for the assessment of pesticide-induced dopaminergic neurotoxicity. *Toxicol In Vitro, 45*(Pt 1), 81-88. doi:10.1016/j.tiv.2017.07.030

James, A. M., Sharpley, M. S., Manas, A. R., Frerman, F. E., Hirst, J., Smith, R. A., & Murphy, M. P. (2007). Interaction of the mitochondria-targeted antioxidant MitoQ with phospholipid bilayers and ubiquinone oxidoreductases. *J Biol Chem, 282*(20), 14708-14718. doi:10.1074/jbc.M611463200

Jauslin, M. L., Meier, T., Smith, R. A., & Murphy, M. P. (2003). Mitochondria-targeted antioxidants protect Friedreich Ataxia fibroblasts from endogenous oxidative stress more effectively than untargeted antioxidants. *FASEB J, 17*(13), 1972-1974. doi:10.1096/fj.03-0240fje

Juarez, J. C., Manuia, M., Burnett, M. E., Betancourt, O., Boivin, B., Shaw, D. E., . . . Donate, F. (2008). Superoxide dismutase 1 (SOD1) is essential for H2O2-mediated oxidation and inactivation of phosphatases in growth factor signaling. *Proc Natl Acad Sci U S A, 105*(20), 7147-7152. doi:10.1073/pnas.0709451105

Kelso, G. F., Porteous, C. M., Coulter, C. V., Hughes, G., Porteous, W. K., Ledgerwood, E. C., . . . Murphy, M. P. (2001). Selective targeting of a redox-active ubiquinone to mitochondria within cells: antioxidant and antiapoptotic properties. *J Biol Chem, 276*(7), 4588-4596. doi:10.1074/jbc.M009093200

Kovalevich, J., & Langford, D. (2013). Considerations for the use of SH-SY5Y neuroblastoma cells in neurobiology. *Methods Mol Biol, 1078*, 9-21. doi:10.1007/978-1-62703-640-5_2

Kumar, P., Nagarajan, A., & Uchil, P. D. (2018). Analysis of Cell Viability by the MTT Assay. *Cold Spring Harb Protoc, 2018*(6). doi:10.1101/pdb.prot095505

Li, H., Zhang, Q., Li, W., Li, H., Bao, J., Yang, C., . . . Jin, H. (2019). Role of Nrf2 in the antioxidation and oxidative stress induced developmental toxicity of honokiol in zebrafish. *Toxicol Appl Pharmacol, 373*, 48-61. doi:10.1016/j.taap.2019.04.016

Ma, Q. (2013). Role of nrf2 in oxidative stress and toxicity. *Annu Rev Pharmacol Toxicol, 53*, 401-426. doi:10.1146/annurev-pharmtox-011112-140320

Martinez, M. C., & Andriantsitohaina, R. (2009). Reactive nitrogen species: molecular mechanisms and potential significance in health and disease. *Antioxid Redox Signal, 11*(3), 669-702. doi:10.1089/ars.2007.1993

Nakagawa, T., Shimizu, S., Watanabe, T., Yamaguchi, O., Otsu, K., Yamagata, H., . . . Tsujimoto, Y. (2005). Cyclophilin D-dependent mitochondrial permeability transition regulates some necrotic but not apoptotic cell death. *Nature, 434*(7033), 652-658. doi:10.1038/nature03317

Piscianz, E., Tesser, A., Rimondi, E., Melloni, E., Celeghini, C., & Marcuzzi, A. (2021). MitoQ Is Able to Modulate Apoptosis and Inflammation. *Int J Mol Sci, 22*(9). doi:10.3390/ijms22094753

Pizzino, G., Irrera, N., Cucinotta, M., Pallio, G., Mannino, F., Arcoraci, V., . . . Bitto, A. (2017). Oxidative Stress: Harms and Benefits for Human Health. *Oxid Med Cell Longev, 2017*, 8416763. doi:10.1155/2017/8416763

Powell, R. D., Swet, J. H., Kennedy, K. L., Huynh, T. T., Murphy, M. P., McKillop, I. H., & Evans, S. L. (2015). MitoQ modulates oxidative stress and decreases inflammation following hemorrhage. *J Trauma Acute Care Surg, 78*(3), 573-579. doi:10.1097/TA.0000000000000533

Prasad, S., Gupta, S. C., & Tyagi, A. K. (2017). Reactive oxygen species (ROS) and cancer: Role of antioxidative nutraceuticals. *Cancer Lett, 387*, 95-105. doi:10.1016/j.canlet.2016.03.042

Rao, V. A., Klein, S. R., Bonar, S. J., Zielonka, J., Mizuno, N., Dickey, J. S., . . . Shacter, E. (2010). The antioxidant transcription factor Nrf2 negatively regulates autophagy and growth arrest induced by the anticancer redox agent mitoquinone. *J Biol Chem, 285*(45), 34447-34459. doi:10.1074/jbc.M110.133579

Senoner, T., & Dichtl, W. (2019). Oxidative Stress in Cardiovascular Diseases: Still a Therapeutic Target? *Nutrients, 11*(9). doi:10.3390/nu11092090

Smith, R. A., & Murphy, M. P. (2010). Animal and human studies with the mitochondria-targeted antioxidant MitoQ. *Ann N Y Acad Sci, 1201*, 96-103. doi:10.1111/j.1749-6632.2010.05627.x

Tu, W., Wang, H., Li, S., Liu, Q., & Sha, H. (2019). The Anti-Inflammatory and Anti-Oxidant Mechanisms of the Keap1/Nrf2/ARE Signaling Pathway in Chronic Diseases. *Aging Dis, 10*(3), 637-651. doi:10.14336/AD.2018.0513

Tufekci, K. U., Civi Bayin, E., Genc, S., & Genc, K. (2011). The Nrf2/ARE Pathway: A Promising Target to Counteract Mitochondrial Dysfunction in Parkinson's Disease. *Parkinsons Dis, 2011*, 314082. doi:10.4061/2011/314082

Vu, H. V., Lee, S., Acosta, T. J., Yoshioka, S., Abe, H., & Okuda, K. (2012). Roles of prostaglandin F2alpha and hydrogen peroxide in the regulation of Copper/Zinc superoxide dismutase in bovine corpus luteum and luteal endothelial cells. *Reprod Biol Endocrinol, 10*, 87. doi:10.1186/1477-7827-10-87

Wang, C. M., Yang, C. Q., Cheng, B. H., Chen, J., & Bai, B. (2018). Orexin-A protects SH-SY5Y cells against H2O2-induced oxidative damage via the PI3K/MEK1/2/ERK1/2 signaling pathway. *Int J Immunopathol Pharmacol, 32*, 2058738418785739. doi:10.1177/2058738418785739

Wang, X., & Michaelis, E. K. (2010). Selective neuronal vulnerability to oxidative stress in the brain. *Front Aging Neurosci, 2*, 12. doi:10.3389/fnagi.2010.00012

Wani, W. Y., Gudup, S., Sunkaria, A., Bal, A., Singh, P. P., Kandimalla, R. J., . . . Gill, K. D. (2011). Protective efficacy of mitochondrial targeted antioxidant MitoQ against dichlorvos induced oxidative stress and cell death in rat brain. *Neuropharmacology, 61*(8), 1193-1201. doi:10.1016/j.neuropharm.2011.07.008

Wei, T., Tian, W., Yan, H., Shao, G., & Xie, G. (2014). Protective effects of phillyrin on H2O 2-induced oxidative stress and apoptosis in PC12 cells. *Cell Mol Neurobiol, 34*(8), 1165-1173. doi:10.1007/s10571-014-0091-4

Werner, C., & Engelhard, K. (2007). Pathophysiology of traumatic brain injury. *Br J Anaesth, 99*(1), 4-9. doi:10.1093/bja/aem131

Xie, H.-r., Hu, L.-s., & Li, G.-y. (2010). SH-SY5Y human neuroblastoma cell line:in vitrocell model of dopaminergic neurons in Parkinson's disease. *hinese Medical Journal, 123*(8), 1086-1092. doi:10.3760/cma.j.issn.0366-6999.2010.08.021

Yan, W., Wang, H. D., Hu, Z. G., Wang, Q. F., & Yin, H. X. (2008). Activation of Nrf2-ARE pathway in brain after traumatic brain injury. *Neurosci Lett, 431*(2), 150-154. doi:10.1016/j.neulet.2007.11.060

Zhong, L., Deng, J., Gu, C., Shen, L., Ren, Z., Ma, X., . . . Yu, S. (2021). Protective effect of MitoQ on oxidative stress-mediated senescence of canine bone marrow mesenchymal stem cells via activation of the Nrf2/ARE pathway. *In Vitro Cell Dev Biol Anim, 57*(7), 685-694. doi:10.1007/s11626-021-00605-2

Zhu, H., Itoh, K., Yamamoto, M., Zweier, J. L., & Li, Y. (2005). Role of Nrf2 signaling in regulation of antioxidants and phase 2 enzymes in cardiac fibroblasts: protection against reactive oxygen and nitrogen species-induced cell injury. *FEBS Lett, 579*(14), 3029-3036. doi:10.1016/j.febslet.2005.04.058

Zhu, Z., Liang, W., Chen, Z., Hu, J., Feng, J., Cao, Y., . . . Ding, G. (2021). Mitoquinone Protects Podocytes from Angiotensin II-Induced Mitochondrial Dysfunction and Injury via the Keap1-Nrf2 Signaling Pathway. *Oxid Med Cell Longev, 2021*, 1394486. doi:10.1155/2021/1394486